การสังเคราะห์สารแขวนลอยของซิงค์ซัลไฟด์ขนาดนาโนและการประยุกต์ใช้ในตัวรวบรวมพลังงานแสงอาทิตย์

นางสาวกนกวรรณ วังโน

วิทยานิพนธ์นี้เป็นส่วนหนึ่งของการศึกษาตามหลักสูตรปริญญาวิศวกรรมศาสตรมหาบัณฑิต
สาขาวิชาวิศวกรรมเคมี ภาควิชาวิศวกรรมเคมี
คณะวิศวกรรมศาสตร์ จุฬาลงกรณ์มหาวิทยาลัย
ปีการศึกษา 2555

SYNTHESIS OF NANO-SIZED ZINC SULFIDE AND ITS APPLICATION IN SOLAR CONCENTRATOR

Ms. Kanokwan Wangno

A Thesis Submitted in Partial Fulfillment of the Requirements
for the Degree of Master of Engineering Program in Chemical Engineering
Department of Chemical Engineering
Faculty of Engineering
Chulalongkorn University
Academic Year 2012

Thesis Title	SYNTHESIS OF NANO-SIZED ZINC SULFIDE AND ITS APPLICATION IN SOLAR CONCENTRATOR
By	Ms. Kanokwan Wangno
Field of Study	Chemical Engineering
Thesis Advisor	Associate Professor Tawatchai Charinpanitkul, Dr.Eng.
Thesis Co-advisor	Wattana Ratismith, Ph.D.

Accepted by the Faculty of Engineering, Chulalongkorn University in Partial Fulfillment of the Requirements for the Master's Degree

…… Dean of the Faculty of Engineering
(Associate Professor Boonsom Lerdhirunwong, Dr.Ing.)

THESIS COMMITTEE

…… Chairman
(Assistant Professor Varong Pavarajarn, Ph.D.)

……. Thesis Advisor
(Associate Professor Tawatchai Charinpanitkul, Dr.Eng.)

……. Thesis Co-advisor
(Wattana Ratismith, Ph.D.)

……. Examiner
(Assistant Professor Apinan Soottitantawat, Ph.D.)

……. External Examiner
(Sitthisuntorn Supothina, Ph.D.)

กนกวรรณ วังโน : การสังเคราะห์สารแขวนลอยของซิงค์ซัลไฟด์ขนาดนาโนและการประยุกต์ใช้ในตัวรวบรวมพลังงานแสงอาทิตย์. (SYNTHESIS OF NANO-SIZED ZINC SULFIDE AND ITS APPLICATION IN SOLAR CONCENTRATOR) อ. ที่ปรึกษาวิทยานิพนธ์หลัก : รศ.ดร.ธวัชชัย ชรินพาณิชกุล, อ. ที่ปรึกษาวิทยานิพนธ์ร่วม : ดร.วัฒนา รติสมิทธ์, 90 หน้า.

ซิงค์ซัลไฟด์เป็นอนุภาคนาโนที่สามารถใช้เป็นวัสดุประกอบร่วมแบบนาโนซึ่งสามารถประยุกต์ใช้งานกับตัวรวบรวมแสงอาทิตย์ซึ่งเป็นอุปกรณ์สำคัญสำหรับเซลล์แสงอาทิตย์ ในงานวิจัยนี้ได้ทำการสังเคราะห์อนุภานนาโนซิงค์ซัลไฟด์โดยใช้วิธีรีเวิร์สไมเซลล์ในการควบคุมขนาดของอนุภาค อัตราส่วนของน้ำต่อสารลดแรงตึงผิว และความเข้มข้นของสารตั้งต้นที่ใช้ในการเกิดอนุภาคนาโน เป็นตัวแปรสำคัญที่ใช้ในการควบคุมขนาดของอนุภาคที่ได้ ซึ่งถูกนำไปวิเคราะห์โดยเทคนิคการวัดความเป็นผลึก (XRD), การถ่ายภาพโดยอิเล็คตรอนแบบส่องผ่าน (TEM), การถ่ายภาพอิเล็กตรอนแบบส่องกราด (SEM), และการวัดค่าความเรืองแสง (PL) พบว่าขนาดของอนุภาคนาโนซิงค์ซัลไฟด์มีผลกับค่าความเรืองแสง นอกจากนี้อนุภาคนาโนยังนำไปประยุกต์ใช้กับวัสดุนำแสงพอลิเมทิลเมธาคีเลต (PMMA) พบว่า ขนาดอนุภาคนาโนที่แตกต่างกันส่งผลต่อค่าความเรืองแสง และส่งผลต่อความสามารถในการเป็นตัวรวบรวมแสงเมื่อประยุกต์ใช้งานร่วมกับเซลล์แสงอาทิตย์

ภาควิชา วิศวกรรมเคมี ลายมือชื่อนิสิต .....

สาขาวิชา วิศวกรรมเคมี ลายมือชื่อ อ.ที่ปรึกษาวิทยานิพนธ์หลัก .....

ปีการศึกษา 2555 ลายมือชื่อ อ.ที่ปรึกษาวิทยานิพนธ์ร่วม .....

5370392121 : MAJOR CHEMICAL ENGINEERING
KEYWORDS : ZNS / PMMA / NANOCOMPOSITE / CONCENTRATOR / MICROEMULSION

KANOKWAN WANGNO : SYNTHESIS OF NANO-SIZED ZINC SULFIDE AND ITS APPLICATION IN SOLAR CONCENTRATOR. ADVISOR : ASSOC. PROF. TAWATCHAI CHARINPANITKUL, Dr.Eng., CO-ADVISOR : WATTANA RATISMITH, Ph.D., 90 pp.

Zinc sulfide has been recognized as a promising nanomaterial which could be applied for solar collector. This work has aimed at synthesis of ZnS nanoparticles by reversed micelle of Triton X-100 and cyclohexane. Molar ratio of water to Triton X-100 and concentration of zinc and sulfide ions play an important role in controlling the size of ZnS nanoparticles. X-ray powder diffraction (XRD), transmission electron microscopy (TEM), scanning electron microscopy (SEM), and photoluminescence spectroscopy (PL) have been used for characterization of the synthesized ZnS nanoparticles. Examination of photoluminescence of the synthesized ZnS nanoparticles reveals its size dependence. In addition, the ZnS/PMMA composites have also characterized by PL and their solar concentrated abilities were also observed.

Department : Chemical Engineering	Student's Signature .....
Field of Study : Chemical Engineering	Advisor's Signature .....
Academic Year : 2012	Co-advisor's Signature .....

ACKNOWLEDGEMENTS

I would like to express my greatest gratitude and appreciation to Associate Professor Dr. Tawatchai Charinpanitkul, my thesis advisor, for his invaluable suggestions, guidance, and encouragement during my study and useful discussions throughout this research. His advice is always worthwhile and without him this work could not be possible.

I sincerely thank Dr. Wattana Ratismith my thesis co-advisor for his helpful suggestions and guidance on my research.

I would like to thank Assistant Professor Dr. Varong Pavarajarn, as the chairman, Dr. Sitthisuntorn Supothina as the external examiner, and Dr. Apinan Soottitantawat as the examiner of the thesis for their valuable guidance and revision throughout my thesis.

I appreciate to the Thai MMA Co., Ltd. for the donation of the most significant chemical.

Thanks to many friends in the Center of Excellence in Particle Technology, Department of Chemical Engineering, Faculty of Engineering, Chulalongkorn University for friendship and their assistance especially the members of powder group. To On-uma Nimittrakoolchai and the many others, not specifically named, who have provided me with support and encouragement, please be assured that I thinks of you.

Finally, I would like to extremely express my highest gratitude to my parents for their unconditional love and their support throughout my study.

CONTENTS

Page

Page

.

LIST OF TABLES

LIST OF FIGURES

Figure Page

Figure Page

CHAPTER I

INTRODUCTION

1.1 Motivation

Effective energy utilization is a very important issue as the world population continuously increases, leading to the elevated need of energy consumption. Many alternative means have been explored to convert energy to more effective utilization. Among some emerging technologies, solar concentration is of interesting regarding to someprevious research works reporting that solar energy concentration can absorb sunlight by the luminescent species and emitted with high efficiency. Such emitted light is trapped in the sheet and travels to the edges where it can be collected by solar cells [1]. However, there still are requirements to improve solar concentrator efficiency for actual applications of photovoltaic or lighting.

Quantum dot solar concentrator (QDSC) is recognized as an application which normally uses some specific semiconductive compounds with confined contentinthreespatialdimensions in nanometer-scaled for a purpose of concentrating influx solar energy [2]. Such quantum dots have electronic properties which are intermediate between those of bulk semiconductors and those of discretemolecules. Many researchers have studied quantum dotsin various aspects, such as transistors,solar cells, light-emitting diode (LED), andso on. Generally, the smaller the size of thecrystal, the greater the difference in energy between the highestvalence bandand the lowest conduction band becomes, therefore more energy is needed to excite the dot[3].

Currently, synthesis of group II-IV semiconductor nanostructure materials have attracted much attention in various fields due to their unique characteristics, which are useful for wide application in catalysis, optoelectronics, microelectronics, magnetics and

biology. Their optical, electronic and magnetic properties are strongly dependent on the sizes and shapes of nanomaterials [4-5].Thiswork aims to synthesize ZnS nanoparticle by microemulsion method. Also, dispersion of ZnS nanoparticle in poly (methyl methacrylate) (PMMA) composite will be examined. Up to now, ZnS nanoparticles have been synthesized by various methods including solvothermal process, solid-liquid method and hydrothermal process. However, some of them require longer processing time or higher temperature and lead to further investigations [6-8]. The microemulsion method is interesting to study.

1.2 Research Objective

This work has set its objective to examine how to synthesize ZnS nanoparticles by microemulsion method and to find the optimum synthesis conditions in order to control particle size of ZnS nanoparticle which would be utilized for preparing composite material with PMMA, to be tested for solar concentrator application. This work has studied the effect of size of synthesis condition which are the molar ratio of water to surfactant (W): 3, 7, 9 and initial concentration on size and photoluminescence propoty of ZnS nanoparticales. Effect of both particle size of ZnS nanoparticles and ratio of the ZnS nanoparticles to PMMA matrix polymer on solar concentrating performance has be also investigated to obtain efficient performance of solar concentrator.

1.3 Research Scopes

The scopes of this research was studied effect of size of ZnS nanoparticle by using microemulsion technique and effect of both particle size of ZnS nanoparticles and ratio of the ZnS nanoparticles to PMMA matrix polymer on solar concentrating performance was also investigated to obtain efficient performance of solar concentrator.

1.3.1 Synthesis of ZnS nanoparticles by microemulsion technique using the following conditions

- Molar ratio of water to surfactant (W): 3, 7, 9

- Concentration of precursor [C]: 0.1, 0.2, 0.5 mol/dm^3

1.3.2 Characterization of the synthesized ZnS nanoparticles with the following techniques:

- Particle size and morphology of the synthesized ZnS will be examined by using transmission electron microscope (TEM) and scanning electron microscope (SEM).

- Crystalline of the synthesized ZnS will be determined by using X-ray diffract method (XRD).

- Photophysical property of the synthesized ZnS will be examined by using photoluminencent method (PL).

1.3.3 Preparation of composite materials of ZnS and PMMA for composits fabricating planar solar collector.

- Characterization of ZnS to MMA (ZnS: MMA=0.003:1 wt/wt) (methylmethacrylate (MMA) accounts for 10 wt% of the total weight), which is a follow technical information of Thai MMA company.

- Composite materials of synthesized ZnS nanoparticles and PMMA.

- Photophysical properties of composite materials will be examined by Photoluminencent method (PL).

- The thin film samples were observed using a scanning electron microscope (SEM)

1.4 Expected benefits

1.4.1 Knowledge of controllable sizes of ZnS nanoparticles by microemulsion.

1.4.2 To understand effects of ZnS nanoparticle characteristics on solar concentrator performance which are fabricated from ZnS-polymethylmethacrylate (PMMA) nanocomposites.

1.5 Procedure

1.5.1 Exploring and review the previous researches.

1.5.2 Designing the experimental method to synthesize ZnS by microemulsion.

1.5.3 Synthesizing ZnS nanoparticles in ternary W/O by microemulsion method.

1.5.4 Mixing ZnS nanoparticles in polymethylmethacrylate (PMMA).

1.5.5 Investigation properties of the composites prepared with various conditions.

1.5.6 Discussion and conclusion of experimental results.

1.5.7 Writing thesis and preparing draft manuscript for journal submission.

CHAPTER II

LITERATURE REVIEWS

The second chapter presents many researches the literature material of about the synthesized ZnS nanoparticles, and application of photoluminescent of ZnS nanoparticles which were interested. The advantages of this method and their applications are summarized in this chapter that is separated in to two part: The first part is the synthesis of ZnS nanoparticles by microemulsion method, which success on the method of controlling of ZnS nanoparticles. The second part presents researches of composite material, which was prepared by mixing ZnS nanoparticles with polymer, and its application as solarconcentratoras.

2.1 Synthesis of ZnS nanoparticles by microemulsionmethod

Wageh et al. (2003) studied about growth and optical properties of colloidal 1.5 nm ZnS nanoparticles. The synthesizing route solution of $Zn(CH_3COO)_2$ $2H_2O$ and mercaptoacetic acid in dimethylformamide (DMF) was adjusted to pH 8 by adding 2M NaOH solution, followed by the drop wise addition of an aqueous solution of sodium sulfide (Na_2S 9H2O) under vigorous stirring in an N_2 atmosphere. The research controlled nanocrystalline size of ZnS nanoparticals by salvothermal they found effect of nanocrystalline size ZnS nanoparticals to photoluminescence, low nanocrystallinnes size has high optical.

Xu and Li (2003) synthesized ZnS nanocrystal in ternary water-in-oil (w/o) microemulsion systems stabilized by either nonionic or, in contrast, cationic surfactant.

They used zinc sulfate and sodium sulfide as the reactant, and CTAB and Triton X-100 as a surfactant. Products were analyzed by transmission electron microscope (TEM) and identified by energy-dispersive X-ray spectroscope (EDS); Electron diffraction (ED) was also performed for individual nanorods. With varying molar ratios of water to surfactant (W_0) in solution, hence changing droplet sizes of water pool of microemulsions consequently, they found that uniform ZnS nanorods could be prepared by using condition W_0=11 at room temperature, incubation time 24 hr, and using Triton X-100 as the surfactant. However, they could only prepare ZnSnanorods with aspect ratio of shape of ZnS nanoparticles by using condition vary water-in-oil [9].

Lay et al. (2004) successfully synthesized ZnS nanowires**,** with diameters around 30 nm and lengths up to 2.5 μm, from solution containing an anionic surfactant, sodium bis(2-ethylhexyl) sulfosuccinate (AOT). Powder X-ray diffraction (XRD) pattern, energy-dispersive X-ray spectroscope (EDS) and selected-area electron diffraction (SAED) pattern indicated that the product was pure polycrystalline cubic-phase β-ZnS. The morphology and size of the as-synthesized product were determined by the TEM. The effects of some of the key reaction parameters (such as the ratio of surfactant to water, the reactant concentration and reaction temperature, etc.) had been explored in this work [11].

Charinpanitkulet al. (2005) synthesized ternary W/O by microemulsion method. They found that the morphology of products could be controlled by W/O. The TEM image of the analysis of the product (Figure 2.1) show different sizes and shape of ZnS nanoparticles which was obtained by varying the (W_0). The effect of co-surfactant on size and morphology of the obtained products have been explored in this work. The key controlling parameters such as the molar ratio of water to surfactant (W_0) and the reactant concentration, which affect the product characteristics, have also been investigated [12].

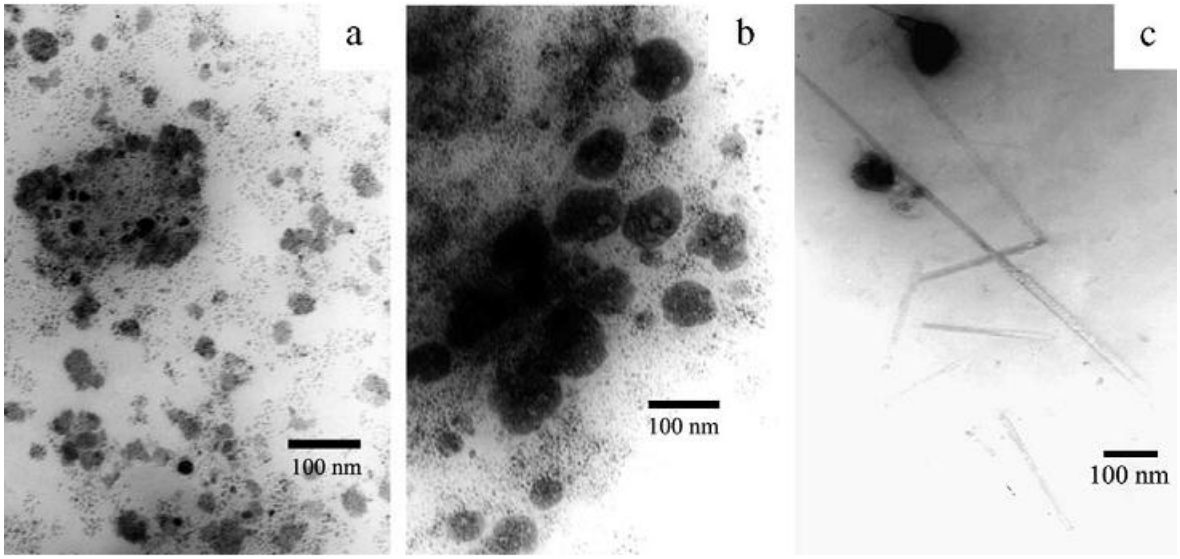

Figure 2.1TEM images of ZnS synthesized at various W_0 (a) 11, (b) 15, and (c) 20 [11]

2.2 Nanoparticles as composite material

Arai et al.(1981) studied ZnSe quantum structures embedded in ZnS which were investigated in a wide range of atomic layer epitaxy (ALE) growth conditions. The optical properties of the grown ZnSe/ZnS quantum structures were studied by PL, photoluminescence excitation (PLE), and cathodoluminescence (CL) spectroscopy. A sharp PL emission is observed at around 3.05 eV, which reveals exciton localization tentatively associated with quasi-OD ZnSe quantum dots [13].

Franco et al.(1981) studied the linear and nonlinear optical properties of organic films based on mixing a polymeric matrix PMMA and a highly nonlinear organic material recently synthesised and characterised, namely(5,50-Bis(3,5-di-tert-butyl-4-oxo-2,5-cyclohexadien-1-ylidene)-5,50-dihydro-2,20-bithiophene),the prospective of reaching a good compromise between good process ability high nonlinear optical (NLO), The properties of the solid solution. Different guest host concentrations have been studied. Due to the high solubility of the guest into the polymeric matrix, we have been able to

reach concentration up to 50% in weight, reaching an enhancement of the NLO properties of PMMA by three orders of magnitudes [14].

Li et al.(1999) studied photophysical properties of ZnS quantum dots**.** They used zinc acetate [$Zn(CH_3COO)_2 \cdot 2H_2O$] and thiourea at 120°C by a solvothermal reaction. The experimental results showed ZnS nanoparticles of ≤ 3 nm average diameter .The UV–Vis spectrum showed an absorption shoulder at 276 nm, corresponding to the bandgap energy of 4.49 eV, and a weak shoulder at 320 nm (3.875 eV) [14].

Rowan and Norton (2006) studied the quantum dot solar concentrator (QDSC) comprising quantum of dots (QDs) seeded in materials such as plastics and glasses, that the QDSC concentrates both direct and diffuse solar energy on attached photovoltaic cells. Spectroscopic measurements have been undertaken for a range of different quantum dot (QD) types and transparent host materials. High transparency in the matrix material and QDs with high quantum efficiency was essential for an efficient QDSC. An optimum matrix material for a QDSC has been determined based on absorption characteristics and an optimum commercially available QD type has been chosen using steady-state absorption, photoluminescence and photoluminescence excitation spectroscopy [15].

Qian et al. (2006) reported alternative-current thin film electroluminescence structure with ZnSe quantum dots embedded in ZnS matrix as light-emitting center, alternative-current electroluminescent spectra. By studying its luminescent spectroscopy and brightness oscillogram of the device, we found that blue emission came from defect states at ZnSe/ZnS interface and the excitation mechanism was hot-electron [16].

Gallagher et al.(2007) studied quantum dot technology to render the concept of a fluorescent dye solar concentrator (FSC) a practical proposition. The quantum dot solar concentrator (QDSC) comprises of quantum dots (QDs) seeded in materials such as plastics and glasses that were suitable for incorporation into building facades.

Photovoltaic (PV) cells attached to the edges convert direct and diffuse solar energy collected into electricity for use in the building of solar cell [17].

Guo and Chen.(2007) reported controllable synthesis of ZnS nanocrystal-polymer transparent hybrids by using polymethylmethacrylate (PMMA) as a polymer matrix. In a typical run, the appropriate amounts of zinc chloride ($ZnCl_2$) and sodium sulfide (Na_2S) in the presence of 2-mercaptoethanol (ME) on play as the organic legend were well dispersed in H_2O dimethylformamide solution without any aggregation. In addition, the Mn-doped ZnSnanocrystals (NCs) were synthesized with similar method. Then, ZnS-PMMA hybrids were obtained via free radical polymerization in situ by using ZnS NCs functionalized with methacryloxypropyltrimethoxysilane (MPS). FT-IR characterization indicates the formation of robust bonding between ZnS NCs and the organic ligand. The TEM images characterized ZnS NCs ,was well dispersed in PMMA matrix, and particle size of as-prepared ZnS NCs is about 2.6 nm, in agreement with the computing results of Brus's model and Debye–Scherrer formula. The photoluminescence measurements present that ZnS NCs, Mn-doped ZnS NCs, and ZnS/PMMA hybrid show good optical properties[18].

Mallet al.(2010) studied the influence of ZnS quantum dots (QDs) on the photo-physical and electrical properties of poly(3-hexylthiophene) (P3HT) conjugated polymer, has been investigated. Composite material has been prepared by blending P3HT with low concentration of chemically synthesized ZnSnanocrystals. Absorption spectra of conjugated polymer exhibit a small blue shift of about 3 nm, with the incorporation of ZnS nanocrystals.This is observed the charge transfer between conjugated polymer molecules and ZnS nanoparticles [19].

CHAPTER III

PRINCIPLES AND THEORYS

3.1 Semiconductor [20]

The semiconductor is material which electrical conductivity is intermediate between that of a conductor and an insulator. The semiconductor materials are crystalline solids. The electron was separated by quanta of energy that called energy band.

3.2 Energy band [20]

Energy bands consisting of a large number of closely spaced energy levels exist in crystalline materials. The bands can be described of as the picking of the individual energy level of electrons enclosing each atom. The electronic energy band was depended crystalline solid which is partially occupied by electrons.

The wave functions of each electrons overlap, was confined to neighboring atoms. The energy band diagram is showed in Figure 3.1.The electronic properties of a semiconductor are controlled by the highest empty band and the lowest filled band; it is often samply to only consider those bands. This leads to simplified energy band diagram for semiconductors as shown in Figure 3.1.

The energy band can be explained from equation 3-1.The equation 3-1 consider ans assembly of N atoms, each with its discrete energy levels, $E\alpha$(i), where i=1,…, N labels the atoms, and bring them together to form a crystal. Let $\Delta E\alpha$ [which is of in the order of order one electron volt (eV)] represents the average spacing of the atom levels.

As the atoms brought together, the electron originally bound to attractive potential of one nucleus begin to interact with the potentials of other nuclei. This shifts each energy level *Eo*and eventually the formerly discrete levels become band of level with an energy spacing.

3.3 Valence band [20]

The valence band is shown Figure 3.1, of including with molecular orbital (MO) theory, that was developed to use the methods of quantum mechanics to explain chemical bonding. It focuses on how the atomic orbital of the separate atoms combine with give chemical bonds when a molecule is formed. In contrast, molecular orbital theory has orbitals that cover the whole molecule. The bonding properties depend on the atomic potentials, that explanation was represented by Schrodinger of wave equation for crystal.

3.4 Conduction band [20]

The conduction band is a range of electron energies that is higher than that of the valence band. The electrons of energy band are increased by going to higher energy levels within the band when an electric field is used to expedite them or when the temperature of the crystal is higher than the surrounding area. These electrons was called conduction electrons, as separated from the electrons in filled energy bands, which, as a whole, do not contribute to electrical and thermal conduction.

The metallic conductors that the conduction electrons correspond to the valence electrons of the constituent atoms. The semiconductors and insulators at sufficiently low temperatures, the conduction band is empty of electrons. Conduction electrons come from thermal excitation of electrons from a lower energy band or from impurity atoms in the crystal. (Figure 3.1)

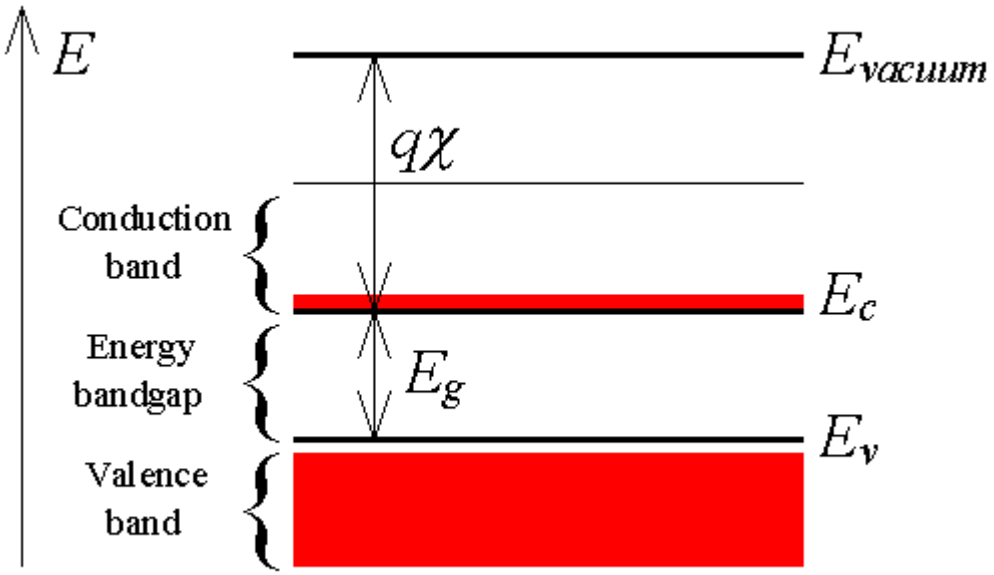

Figure 3.1 simplified energy band diagram used to describe semiconductors. [2]

3.5 Quantum well [22]

Quantum well is potential well with only discrete energy values. Quantum wells use direct optical transitions in semiconductor technology. The technology is produced quantization which confine particles, originally free to move in three dimensions, to two dimensions, forcing them reside a planar region. The effects of quantum were limited take place when the quantum well thickness becomes comparable to the de Broglie wavelength of a carriers (generally electrons and holes), leading to energy levels called "energy sub bands". The carriers can only have discrete energy values. In order for the most important semiconductor devices to function at their present levels, similar high levels of interfacial perfection are required. For bulk crystals we now know that the chief reason why semiconductors are superior to other materials. The zero-dimensional was respected by topological space , that the equivalent notions of specific a dimension to

given topological space. Specifically, a topological space is zero-dimensional with respect to the Lebesgue covering dimension if every open cover of the space has a refinement which is a cover of the space by open sets such that any point in the space is contained in exactly one open set of this refinement as shown in Figure 3.2.

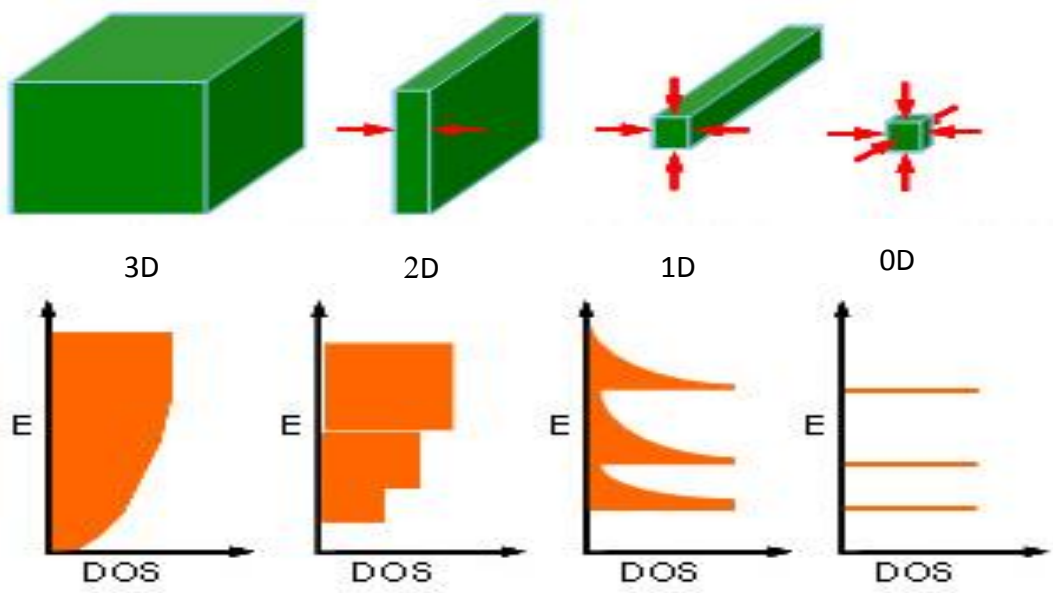

Figure 3.2 Dimension and energy of material. [23]

3.6 Fundamental optical spectra [24]

Almost all our well known of the electronic structure of atoms come from spectroscopic studies of line spectra. The proportion of our knowledge of the electron structure of semiconductor system from theoretical analysis of optical reflectivity from clean crystalline surfaces. While the spectral structure of atom.

3.7 Basis for absorbance spectrophotometry [25]

The basis of the spectrometer explain about propertied light scattering as follow:

Beer's Law: A αc and A αb

so Aα b ×c

A = a × b×c proportionality constant absorptive units of L/g·cm.

If units of concentration are M (mol/L) then use molar absorptive ε (units of L/mol·cm)

A = ε× b ×c.

Phenomena used for optical measurements Absorption, Emission, Luminescence (Fluorescence, Phosphorescence, Chemiluminescence), Scattering.

In all cases, response is proportional to concentration of analyze. As show in Figure 3.3

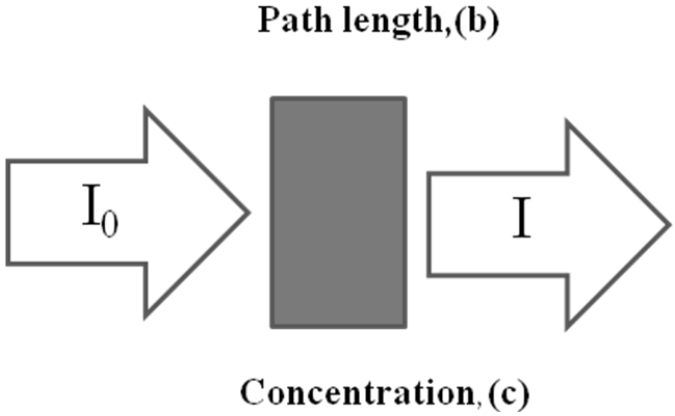

Figure 3.3 Optical Spectroscopy and Instrumentation [25]

Transmittance	$T = I / I_0$	(3-2)
Percent Transmittance	$\%T = I / I_0 \times 100\%$	(3-3)
Absorbance	$A = -\log T = -\log(I / I_0)$	(3-4)

3.8 Photoemission [24-26]

The photoelectric effect measured electrons emitted energy from solids, gases or liquids by the photoelectric effect. The binding energies is determine of electrons in a substance. When the electron is excited from a state in the valence band to a state in the

conduction band by absorbing a photon, it may escape from the crystal if its energy in the final state lies above the vacuum level. The level lies well above the most of the conductions band state near the energy gap, and of course it is these agates which are of greatest interest. In addition most of the electron which escape from the crystal without inelastic scattering were excited quite close to surface, so the surface preparation, which was already critical for ordinary optical measurement become even more critical photoemission experiment.

Regardless of the incident photon beam however, all photoelectron spectroscopy revolves around the general theme of surface analysis by measuring the ejected electrons. The energies of the emitted photoelectrons are original electronic states, and depend on vibration state and rotational level.

The photoelectrons could escape only from a depth on the order of nanometers, so that is the surface layer which is analyzed, that is high frequency of the light, and the many charge and energy of emitted electrons. The photoemission is the most sensitive and accurate techniques for measurement, that energies and shapes of electronic states and molecular and atomic orbital. Photoemission is the most sensitive methods of detecting substances in trace concentrations, provided the sample is compatible with ultra-high vacuum and the analyst can be distinguished from background. This is achieved by applying Einstein's relation.

The *hv* term of this equation is due to the energy (frequency) of the UV light that bombards the sample. Photoemission spectra are also measured using synchrotron radiation sources.The binding energies of the measured electrons are characteristic of the chemical structure and molecular bonding of the material. By adding a source monochromator and increasing the energy resolution of the electron analyzer, peaks appear with full width at half maximum (FWHM) less than 5–8 meV.

3.9 Hole energy levels and optical transitions in real semiconductors [27]

The valence band near wavenumber equal to zero in most semiconductors contains two branches corresponding to the heavy and light holes, and the 3rd branch splits off because of spin-orbit interaction. Furthermore, in a number of absolute value of the materials of the hole effective mass are different for each direction. So, the quantum confinement is considered to effect in the valence band of real semiconductors which ought to be made with the complex structure. The hole kinetic energy operator should be included in the Luttinger Hamiltonian correlation [28]. In the case of a spherical symmetric can be expressed by A.Baldereshi and N. Lipari (1973) [29].

$$H_h = \frac{\gamma_1}{2m_0}\left[\hat{P}^2 - \frac{\mu}{9}\left(P^{(2)}J^{(2)}\right)\right] \qquad (3\text{-}5)$$

Where J is the angular momentum operator

$P(2)$ and $J(2)$ are the second rank tensor operator

$\mu = (6\gamma_3+4\gamma_2)/5\gamma_1$

γ_i = Luttinger parameters.

An analysis of the Schroedinger equation with the hole kinetic energy in this expression and with the electron kinetic energy in the form relevant to a free particle leads to an important modification of hole energy levels and the diagram of optical transitions [30-32]. The hole wave function expressed as in linear combinations of the different valence states and has mixed symmetry. The spectra of the electron-hole and the probabilities of the optical transition have been determined derived from *precise equation*

for the case of GaAs [33], CdS [34], Si [35], CdSe [36], and CdTe [37]. An example for the optical spectrum and the relevant for GaAs quantum dots were shown in Figure 3.4.

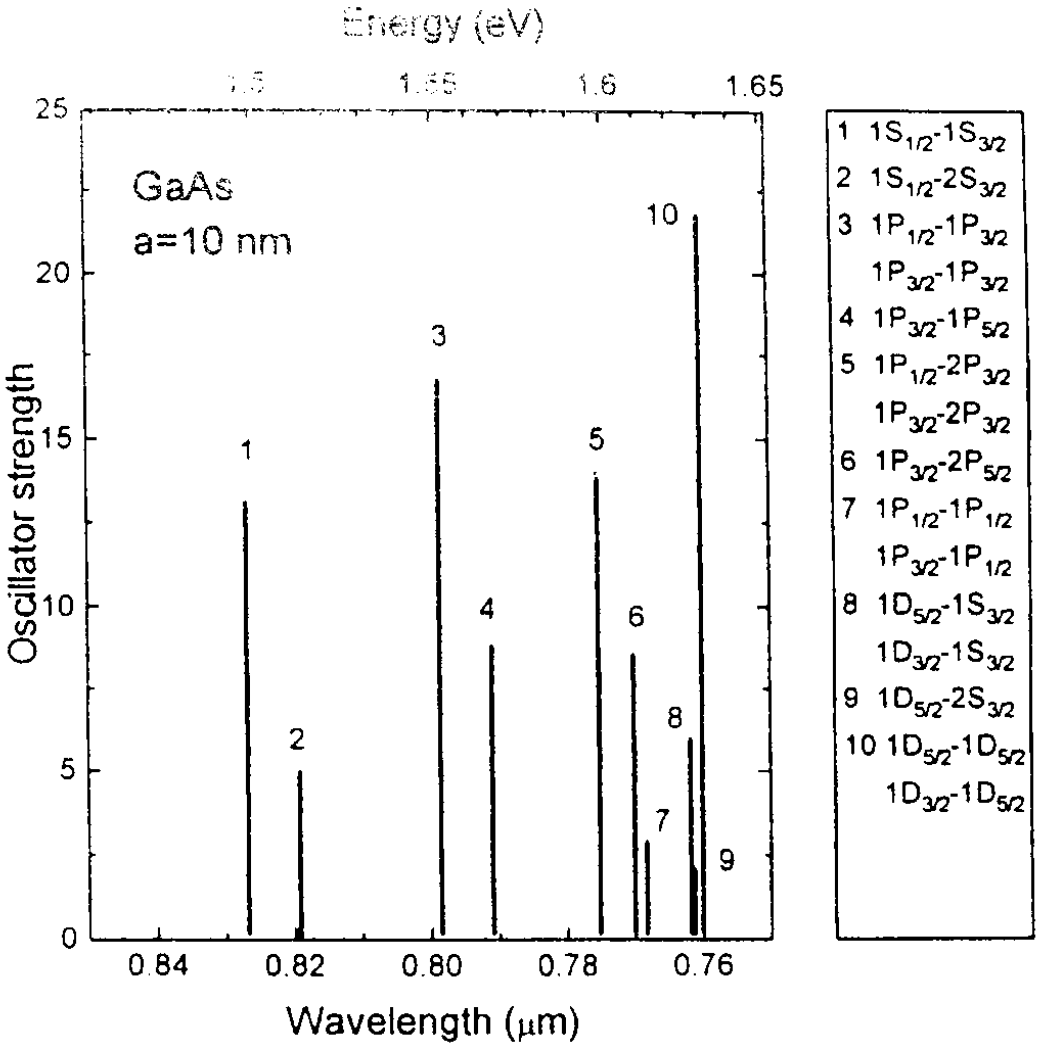

Figure 3.4 Oscillator strengths of the first 10 absorption resonances of GaAs quantum dot (a = 10 nm) calculated by J. Pan (1992) [27]

3.10 Size-dependent [27]

The effective mass approximation gives an electronic properties description of nanocrystals on the way from crystal like to cluster like behavior. It can predict a number of size dependent features due to the three-dimensional spatial confinement of quasi-particles. The main appearance of quantum-size effects is the continuous blue shift of the

absorption with decreasing size of nanocrystals. The size-dependent band gaps for a number of semiconductor materials are presented in Figure3.5 to give an idea concerning absolute values of the effect. Crystal contains less than 10^3 atoms for a quantum dot radius less than 2 nm.

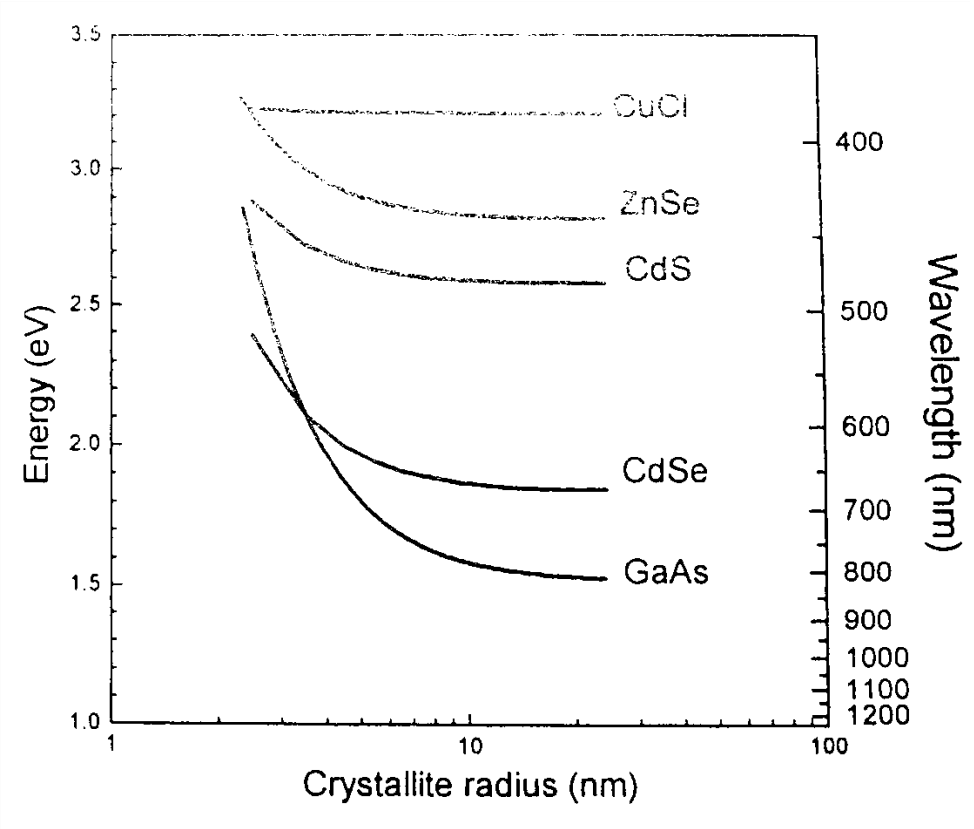

Figure 3.5 Energy of the absorption and calculated crystallite size [27]

One possible correction to this approach is to assume that the energy dependence of the effective mass non-parabolicity of the bands, when kinetic energy of confined quasi-particles moves from the band extremism [38]. Another possibility is to be the empirical pseudo potential method in which the exact crystal-field potential experienced by the valence electron is replaced by an effective potential. This method is used for band

structure calculations of bulk crystals and has been successfully applied to nanocrystals [39].

The size ranges for semiconductor nanocrystals related to different models and approaches, which provide an adequate description of their optical properties. The characteristic length parameters to be involved in such a classification are the crystal lattice constant, a_L, the exciton Bohr radius, a_B, and the photon wavelength λ corresponding to the lowest optical transition. If the size of a nanocrystal is comparable to a_L and adequate description can be provided only in terms of the quantum-chemical (molecular) approach with the specific number of atoms and configuration taken into account. This size interval can be classified as a cluster range. The main distinctive feature of clusters is the absence of a monotonic dependence of the optical transition energies and probabilities versus number of atoms. The size as a characteristic of clusters is by no means justified. A subrange can be outlined corresponding to surface clusters in which every atom belongs to the surface. This type of cluster possesses an enhanced chemical activity

3.11 Synopsis of nanocrystals fabricated by various techniques [40]

Many types of substances have been used to fabricate nanocrystals possessing the absorption edge from the near ultraviolet (e.g., CdS in the strong confinement limit and CuCl in a weak confinement regime) to the infrared region (e.g., PbS in the strong confinement regime). The examples of the nanocrystal II-VI pairs were summarized in the Table 3.1.

Table 3.1 II-VI nanocrystals developed by various techniques [40]

Nanocrystals	Environment	References
CdS	Silicate glass	Ekimov, Efros, and Onushchenko 1985 [41]
		Potter and Simmons 1988 [42]
		Liu and Risbud 1990 [43]
	Aqueous solution	Rossetti Nakahara, and Brus 1983 [44]
	Polymer	Weller et al. 1986 [45]
		Misawa et al. 1991 [46-47]
		Woggon, Bogdanov et al. 1993 [48]
		Murray, Norris, and Bawendi 1993 [49]
	Sol-gel glass	Nogami, Nagasaka, and Takata 1990 [50]
		Minti et al. 1991 [51]
		Spanhel, Arpac, and Schmidt 1992 [52]
		Mathieu et al. 1995 [53]
	Zeolite	Wang et al. 1989 [54]
	Semiconductor-glass composite film	Gurevich et al. 1992 [55]
CdSe	Silicate glass	Ekimov, Efros. And Onuschchenko 1985 [41]
		Borrelli et al. 1987 [56]
		Gaponenko, Woggon, and Saleh et al. 1993 [57]
	Polymer	Bawendi et al. 1989 [58]
	Polycetstalline film	Murray, Norris, and Bawendi 1993 [59]
CdTe	Silicate glass	Hodes et al. 1987 [60]

		Potter and Simmons 1990 [61]
	Semiconductor-glass	Liu et al. 1991 [62]
	composite film	Ochoa et al. 1996 [63]
	Polymer	
		Murray, Norris, and Bawendi 1993 [59]
$CdTe_xS_{1-x}$	Silicate glass	Bandaranayake et al. 1995 [64]
ZnSe	Polymer	Neto et al. 1991 [65]
	Polycrystalline film	Chestnoy, Hull, and Brus 1986 [66]
ZnS	Polymer	Goncharova and Sinitsyn 1990 [67]
ZnS:Mn	Polymer	Kortan et al. 1990 [68]
CdZnSe	ZnSe	Bhargava et al. 1994 [69]
HgS	Composite film	Illing et al. 1995 [70]
(Zn, Cd) Se	ZnSe surface	Zylberajch, Teixier, and Barraud 1989 [71]
		Lowisch et al. 1996 [72]

3.12 Microemulsion principle and its component [73-78]

Microemulsions are isotropic liquid mixtures of oil, water and surfactant, frequently in combination with a cosurfactant. The aqueous phase may contain salt(s) and/or other ingredients, and the oil may actually be a complex mixture of different hydrocarbons and olefins. In contrast to ordinary emulsions, microemulsions form upon simple mixing of the components and do not require the high shear conditions generally used in the formation of ordinary emulsions. The three basic types of microemulsions are direct (oil dispersed in water, o/w), reversed (water dispersed in oil, w/o) and bicontinuous.

In ternary systems such as microemulsions, where two immiscible phases (water and ‘oil’) are present with a surfactant, the surfactant molecules may form a monolayer at the interface between the oil and water, with the hydrophobic tails of the surfactant molecules dissolved in the oil phase and the hydrophilic head groups in the aqueous phase.

Surface active agents or surfactants are known as amphiphilic molecules. They have both polar and non-polar characteristics in the same molecule. Therefore, a surfactant molecule has both hydrophiphobic (water-loving) and hydrophilic (water-hating) components. Symbolically, a surfactant molecule can be represented as having a polar “hydrophilic head” and a non-polar “hydrophobic tail” Surfactant could be categorized into the following classifications according to the nature of the hydrophilic group: Anionic: hydrophilic head is negatively charged. Cationic: hydrophilic head is positively charged. Nonionic: hydrophilic head is polar but not charged. Zwitterionic: molecule has both potential positive and negative groups; charge depends on pH of the medium.

The amphiphilic nature of surfactant molecules causes them to accumulate at interface of liquid. Furthermore, surfactant molecules can self-assemble into dynamic aggregates known as micelles. The surfactant concentration at which the first micelle is formed is known as the critical micelle concentration (CMC). Beyond the CMC, any surfactant added to aqueous solution does not increase the number of surfactant monomers in aqueous solution, but rather will contribute to the formation of addition micelle.

As mentioned above, microemulsions are isotropic, thermodynamically stable dispersions of oil, water, surfactant and often cosurfactant (with is generally alcohol). Microemulsion can be characterized as oil-in-water (O/W), water-in-oil (W/O) or

bicontinuous system. Oil-in-water is microemulsion in equilibrium with an excess oil phase with the surfactant molecules existing in the aqueous phase in form of normal micelles. On the other hand, water-in-oil (W/O), microemulsion that coexists with an excess water phase and the surfactant molecules which aggregate in the oil phase in the form of reverse micelle.

Microemulsions have been used as chemical reactors because of their special interfacial properties allowing an intimate contact, at nanoscale level, of hydrophilic and hydrophobic domains. In microemulsions, the size of droplets is in a range of 10-100 nanometers. When interactions among droplets occur, some droplets will coalesce and then spontaneously break apart. There must be a balance of forces present to drive the coalesced micro-emulsion droplets into splitting again. Overtime, the average droplet size of a micro-emulsion will remain constant. This results in a mixing of the contents inside the microemulsion droplets.

There are generally asked “What a microemulsion droplet looks like”, and what its dynamic behavior is? It is helpful to think of a microemulsion droplet as an intermediate between a micelle and an emulsion droplet. Some researchers even suggest that a W/O microemulsion droplet to be a hydrated reverse micelle. One can consider an emulsion droplet to be a rather static structure, a large droplet of water suspended in a continuous phase of oil, with the oil/water interface stabilized by a monolayer of surfactant. On the other hand, a micelle is a very dynamic structure. It is a bit deceiving to see drawings of micelles in journals, because this representation is by necessity static, and micelles are actually dynamically changing and loosely bound aggregates. There is equilibrium and a constant exchange between surfactant monomers and surfactant in the micelle aggregation. Micelles may have lifetimes as short as milliseconds, while emulsion droplets have long lifetimes, without the disintegration we see in micelles, but potentially

with the occurrence of some coalescence over time. Given these two extremes of micelles and emulsion droplets, what our model for microemulsion droplets will be. It is known that the contents of mixed microemulsions do, this allows reactions to occur using microemulsion droplets as tiny microreactors. Because the water droplet is very small, we knew that there exist two significant states of water, the “free” water in the interior of the droplet, and the water at the interface, associated with the surfactant molecules. Since we know that some fraction of microemulsion droplet collisions result in coalescence, yet the mean droplet size in the microemulsion remains constant over time, there must be a driving force to break up these aggregations again. Positive interfacial tension is the driving force for decreasing interfacial area of a giving droplet, so there must be some “negative” interfacial tension present to force an increase in interfacial area and the resulting breakup of microemulsion droplets that are too large. At the optimum droplet size, the forces are balanced and the interfacial tension must approach zero. We can envision a microemulsion as a dynamic entity, a tiny droplet surrounded by a monolayer or aggregate of surfactant, sometimes combining with its neighbors, and subsequently breaking apart, sometimes exposing the water phase to the oil phase.

Microemulsion nonionic surfactants. For oil-in-water (O/W) microemulsions made with ionic surfactants, the primary force preventing coalescence is electrostatic charge repulsion. These microemulsions display the greatest ability to solubilize one phase within another. For W/O microemulsions, and microemulsions made with nonionic surfactants, there is only steric hindrance preventing coalescence of the droplets. This is a weaker force than electrostatic repulsion, so these microemulsions display less solubilization ability. Steric hindrance is affected only by the part of the surfactant molecule exposed to the continuous phase, for example, the hydrophobic region in a W/O microemulsion. Repulsion is enhanced by the of this region, as well as disorder

introduced by such features as double bonds, which introduce bends and interfere with orderly packing of the surfactant molecules at the interface.

As mentioned above, microemulsions have been used as chemical reactors because of their special interfacial properties allowing an intimate contact, at nanoscale level, of hydrophilic and hydrophobic domains. There are many parameters which effect on a size and a morphology of nanoparticles synthesized in microemulsion. How does each micelle move, and how often micelle can contact to the other? If one assumes that microemulsion domains are formed by spherical droplets, the characteristic droplet's collision time in microemulsions can be easily calculated assuming that the droplets diffuse through a continuous medium with viscosity, η.

3.13 Polymerization [79-80]

The polymerization is process of reacting monomer molecules together in a chemical reaction to form polymer chains or three-dimensional networks. A product was combined by chemical, which a very large chain is a network molecule. Many thousands of monomer molecules must be combined to make a product, which has certain unique physical properties, such as, elasticity, high tensile strength, or the ability to form fibers.

The reaction mechanisms of chemical compounds occurs via a variety of polymerization, that complexity occurs a functional groups present in reacting compounds.

Step-growth polymers are specified polymers formed by the stepwise reaction between functional groups of monomers, usually containing heteroatoms. The most step-growth polymers are classified as condensation polymers, but not all step-growth polymers (like polyurethanes formed from isocyanate and alcohol bifunctional

monomers) release condensates. The addition polymers of step-growth is increased of molecular weight, which a very slow rate is lower conversions and reach fairly high molecular weights. This method is adjusted definitions for condensation and addition polymers have been developed. A condensation polymer is defined as a polymer, that concern loss of small molecules during its synthesis. as shown in Figure 3.6.

Chain-growth polymerization (or addition polymerization) deal with the linking together of molecules incorporating double or triple carbon-carbon bonds, that well known monomers have extra internal bonds which are able to break and link up with other monomers to form the repeating chain. Chain-growth polymerization is a involved in the manufacture of polymers such as polyethylene, polypropylene, and polyvinyl chloride (PVC). A special case of chain-growth polymerization leads to living polymerization.

The polymerization radical is portaged center like the one that attacked depends on the specific type of addition mechanism. There are several mechanisms through which this can be initiated. The free radical mechanism is one of the first methods to be used. Free radicals are very reactive atoms or molecules that have unpaired electrons.

There is linear polymerization process. As showFigure 3.6, that is a group of bifunctional (f=2) monomers reacting of a step-growth polymerization due to the kinetic behavior of the different polymerization mechanisms. On a step-growth reaction there are two different ways to create a tetra monomer or a penta monomer. Three different reaction steps can create a hexamer and a heptamer, and forth. In contrast, during chain-growth polymerizations the monomers can only react with active sites forcing the reaction to proceed by only one

3.14 Fundamentals of ZnS synthesis by microemusion method

The miccroemulsions are isotropic, thermodynamically stable dispersions of oil, water, surfactant and often cosurfactant. Microemulsion can be characterized as oil-in-water (O/W), water-in-oil (W/O) or continuous system. Oil-in-water is microemulsion in equilibrium with an excess oil phase with the surfactant molecules existing in the aqueous sphase in form of normal micelles. On the other hand, water-in-oil (W/O), microemulsion that coexists with an excess water phase and the surfactant molecules which aggregate in the oil phase in the form of reverse micelle. The micelles are surfactant molecules, that the typical micelle in aqueous solution forms an aggregate with the hydrophilic "head" regions in contact with surrounding of water, and the hydrophobic " tail " regions in contact of oil as shown in Figure 3.7.

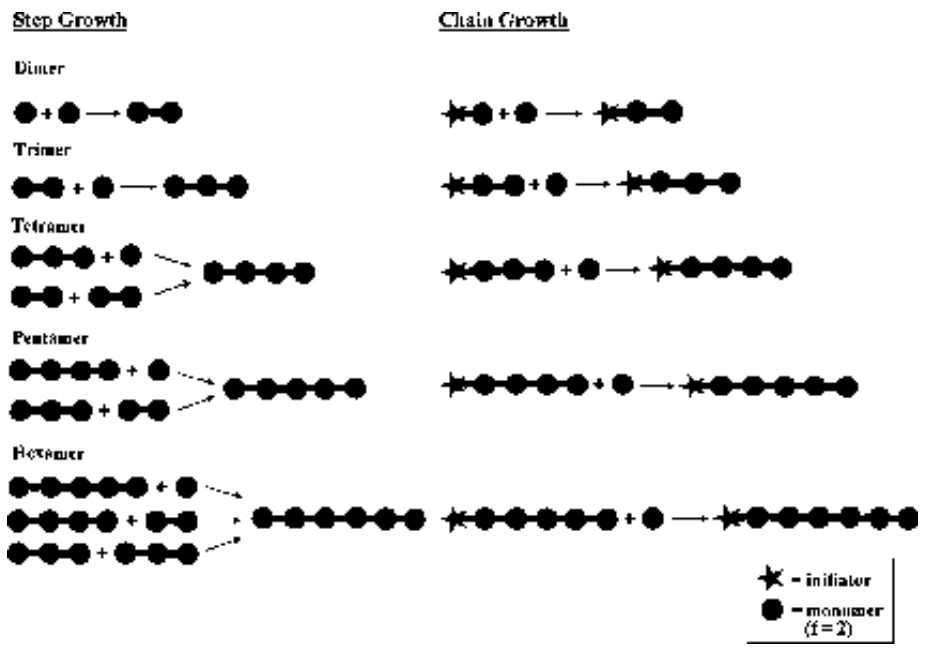

Figure 3.6 Comparison between a step-growth and chain growth polymerization. [80]

The microemulsions method can controll size by surfactant molecule.The surfactant can limit a regions of oil and water, When the system has many surfactant, that

will be the system of microemulsion was small particles of about 10-100nm . The surface was of water droplets to form tiny “pools” dispersing in oil surroundings. The mixing of two “pools” containing different reactants results in constantly collisions between water droplets and eventually leads to a desired chemical reaction accompanied by nucleation and growth processes [81].

3.15 Fundamentals of ZnS/PMMA nanocomposite

ZnS nanoparticles could be employed in a fluorescence solar concentrator (FSC) similar to luminescent dyes as conceptually shown in Figure 3.8. Electron in ZnS nanoparticles are able to desorbs photo energy of solar concentrator due to the advantage of its nanoparticle size which is in the same wavelength of electron. This is known as De Broglie wavelength of electron [82].

When the solar light incidents at the surface of the translucent medium, the visible light will penetrate and refract in the medium and then adsorbed by polymer, the matrix phase. Therefore, nanomaterials release low frequency photon energy. The released photon energy has no refraction to the air, in addition, all photon reflect at the inside surface of the translucent material, which cause to accumulation of the photon energy inside the concentrator and, then, transport to the connected solar cell.

Some previous research reported that the efficient concentrator needs to have some particular characters. The great specifications are the high transparency, suitable size of nanoparticles which contribute to suitable of the energy adsorption and desorption of photon. All of the reflected solar energy could be adsorbed in the medium and the released photon could be specified their path ways in small length.

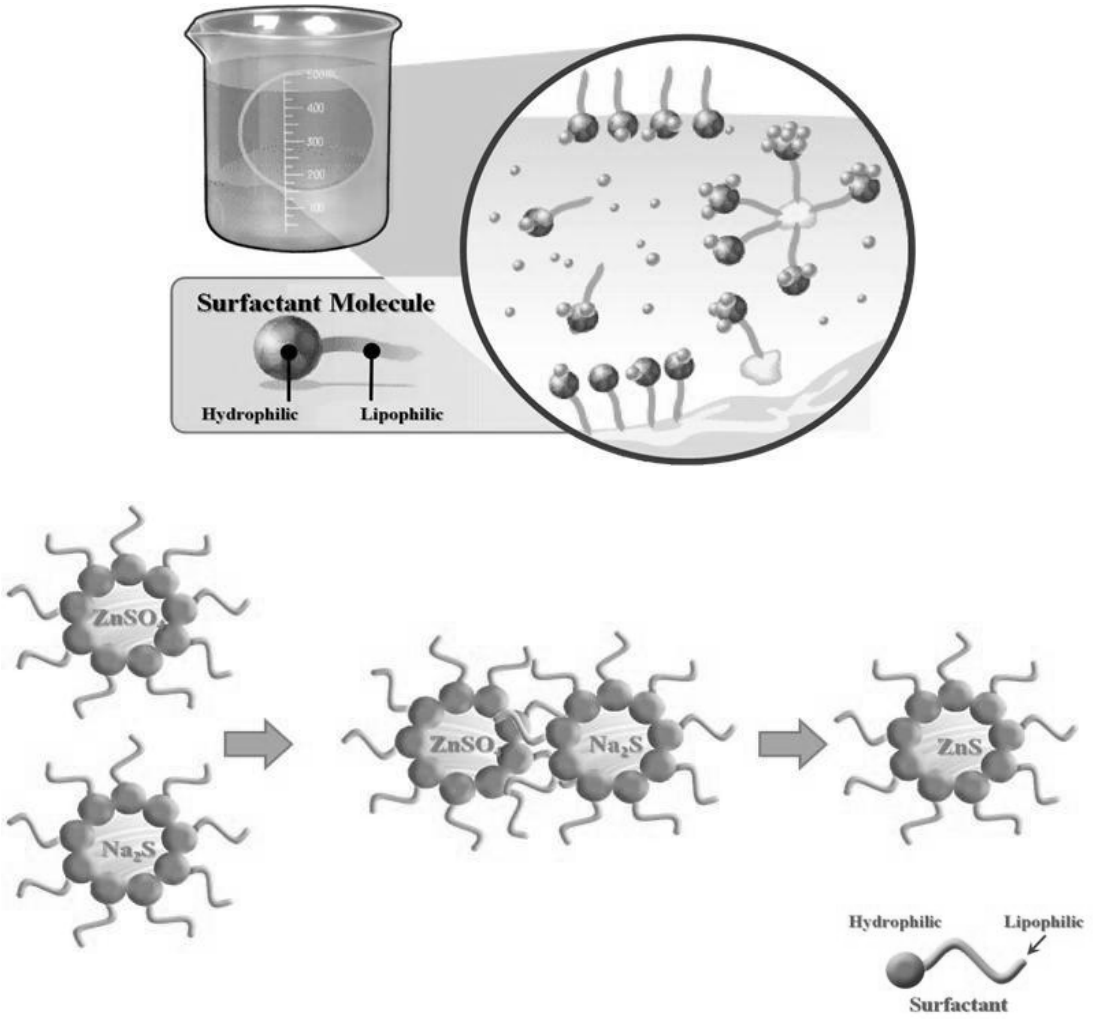

Figure 3.7 Model of micelle in microemulsion method [81]

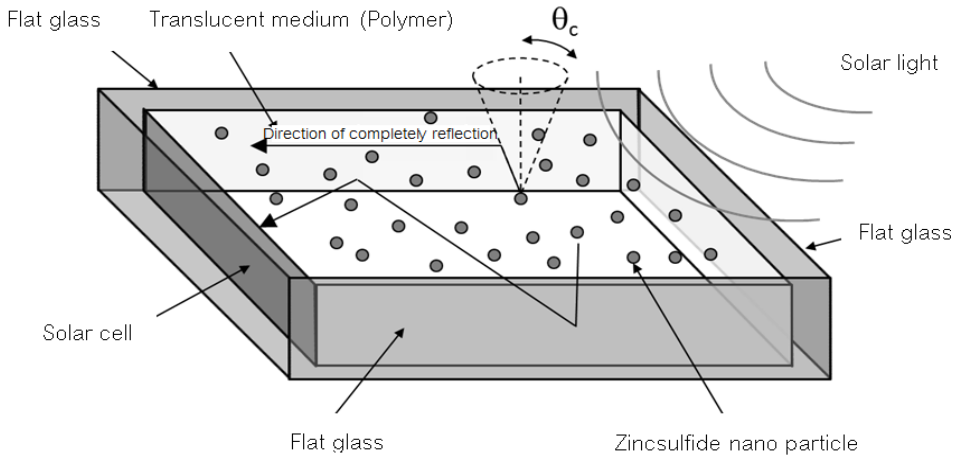

Figure 3.8 Concept of solar concentrator comprising of ZnS nanoparticles [82]

Therefore, nanomaterials used for comprising with the concentrator, could be individualized solar adsorption and photon releasing characteristics that appropriate with the solar cell operating and further characteristics could be toughened and stabilizing with chemicals. From pre-experimental and previous reports, ZnS nanoparticle would provide the highest performance because of its suitable characteristics as mentioned above.

The choosing of the medium material must be importantly considered to the adsorption ability. The material should have a low adsorption coefficient, a soluble property, a good reflection when comprise with nanoparticle, chemicals inertness, low cost productivity, and poison less. A typical material is engineering plastics such as polymethyl methacrylate which has better transparency than glass and easily fabricating. The polymer is usually fabricated in types of sheet or cylinder.

As mentioned above, the ZnS/PMMA camposites material has prominent abilities in adsorption and releasing of solar energy which is affected by size and shape that differentiate through the synthesizing parameters. The synthesized particle is utilized by comprising with the good transparency and ease fabricating material, the polymethyl methacrylate. Therefore, it is strongly believed strongly believe that this research project is possible to develop the higher performance concentrator by modifying with ZnS nanoparticles.

CHAPTER IV

EXPERIMENTAL AND ANALYSIS

4.1 Experimental

All experiments can be separated into two parts. The first part was synthesis of ZnS nanoparticles via microemulsion method. In this part, the molar ratio of water to surfactant (W) and concentration of precursor (C) were varied. The second part was preparation of nanocomposite material by means of dispersion of the obtained ZnS powder in polymethylmethacrylate (PMMA).

All the synthesized ZnS nanoparticles were characterized by Scanning eletron microscopy (SEM), X-Ray diffraction spectroscopy (XRD), Transmission electron microscopy (TEM), and Photoluminescent spectroscopy (PL). The ZnS nanoparticles/PMMA films were characterized by SEM, Photoluminescent (PL) Spectroscopy, and Solar concentrator- nanocomposite film energy producing ability.

4.2 Synthesis of ZnS nanoparticle by microemulsion technique

In this research, chemicals were used as follows:

1. Zinc sulfate ($ZnSO_4$)
2. Sodium sulfide (Na_2S)
3. DI water
4. Cyclohexane
5. Triton X-100
6. Octanol

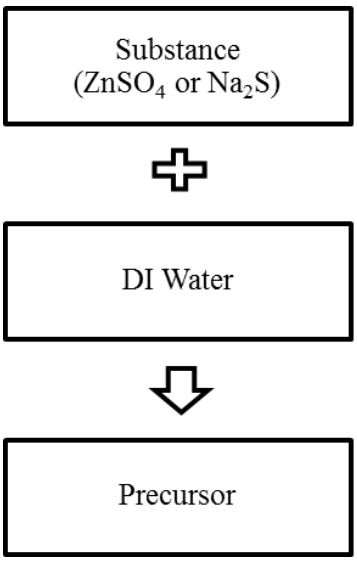

Figure 4.1 Precursor preparation

The microemulsion procedure for ZnS synthesis is shown in Figures 4.1 and 4.2. To prepare the precursors, a designated amount of substance ($ZnSO_4$ or Na_2S solid) was dissolved into water to give a precursor concentration (C) of 0.1, 0.2 or 0.5 M and stirred for 1 h (named as C01, C02 or C05). A specify amount of the precursors (W) of 3, 7, or 9 was dropped slowly into each beaker contained with a mixture of 14 ml of Triton X-100 (surfactant), and 50 ml of cyclohexane (oil phase) and the mixtures were then stirred for 1 h. After stirring, each mixture was dropped with 3.8 ml of n-octanol (cosurfactant) and stirred for 1 h at room temperature. Then the two microemulsions were mixed and stirred for 1 h and rested for 10 h. The ZnS nanoparticles were washed and filtered for three times by ethanol to remove surfactant. The synthesized ZnS particles were named respecting to their synthesized conditions as shown in Table 4.1.

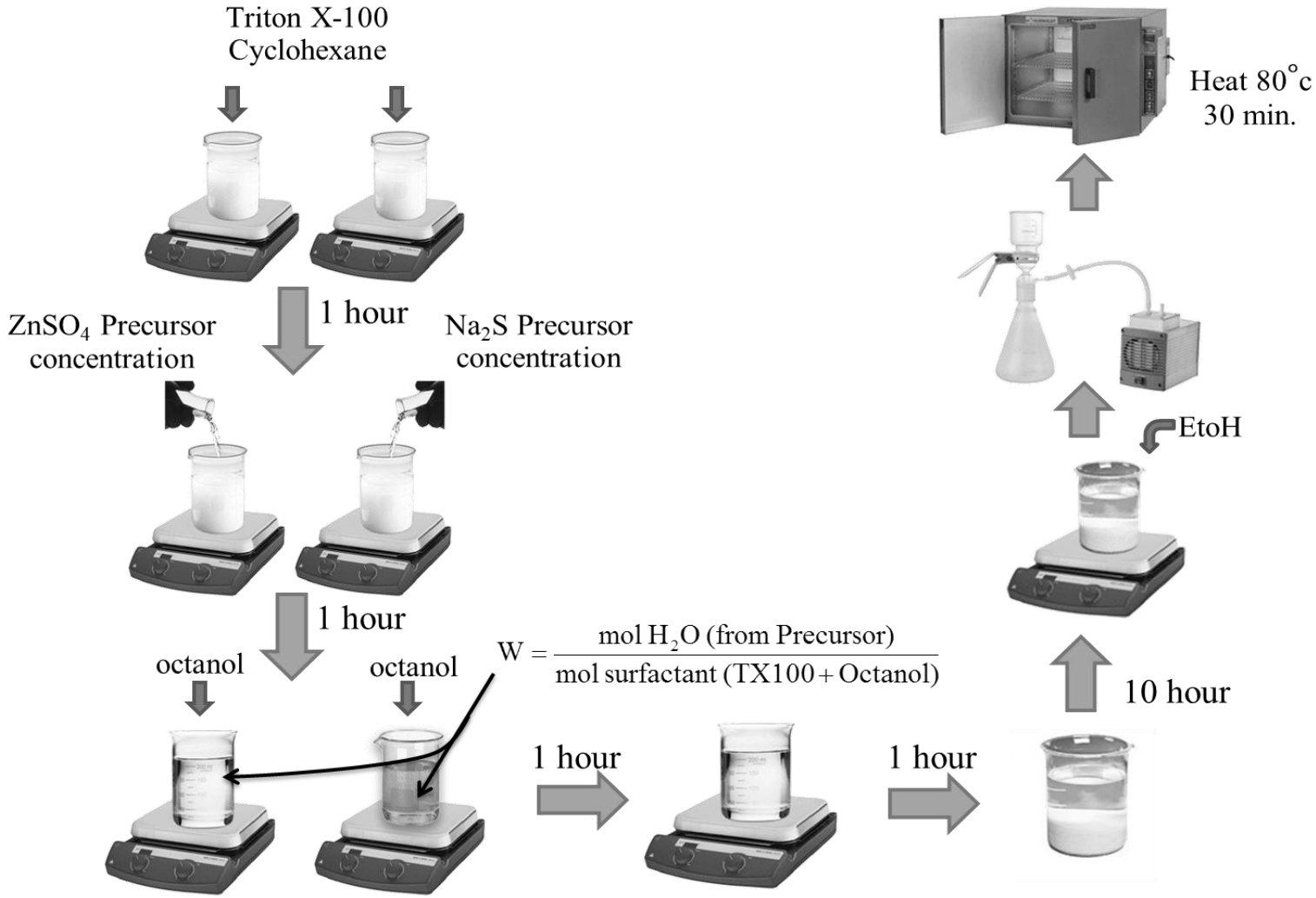

Figure 4.2 Systhesis of ZnS nanoparticle by microemulsion method

Table 4.1 Nomenclature of the ZnS particle

Precursor concentration (C)	Water to surfactant molar ratio (W)	ZnS Nomenclature
0.1	3	C01W3
0.1	7	C01W7
0.1	9	C01W9
0.2	3	C02W3
0.2	7	C02W7
0.2	9	C02W9
0.5	3	C05W3
0.5	7	C05W7
0.5	9	C05W9

4.3 Preparation of ZnS/PMMA nanocomposite

This experimental section used the materials as followed:

1. ZnS powder
2. Methyl methacrylate (MMA, courtesy of Thai MMA Co.,Ltd.)
3. Syrup polymethyl methacrylate (PMMA 28%, courtesy from Thai MMA Co.,Ltd.)

The ZnS/PMMA nanocomposite film was prepared via in situ polymerization of ZnS and MMA. Firstly, the syrup was vacuumed for 30 min at room temperature in order to remove the oxygen. The 0.003 g of ZnS powder and 0.5 g of MMA were mixed and sonicated for 30 min. Then, the ZnS/MMA suspension was added and mixed with the 1 g of syrup and sonicated for 30 min. The final suspension was pulled with micropipet for 0.5 ml and dropped on a glass slide and spread out with doctor blade. The film was rested for 12 h. The procedure was repeated with 0.006 and 0.012 g of ZnS powder. The

ZnS/PMMA sheet was prepared at Thai MMA Co.,Ltd. The procedure to prepare it was in confidential.

4.4 Analytical technique

The morphology and size of the synthesized ZnS were analyzed by SEM (JEOL JSM 5410 LV) and TEM (JEOL JEM-1230). Elemental analysis and crystalline phase of samples were analyzed by EDS and XRD respectively. The photophysical of the synthesized ZnS was analyzed by Photoluminesce (PL) and UV-vis spectroscopy.

4.4.1 Scanning electron microscopy (SEM)

The scanning electron microscopy (SEM) is extremely useful for imaging surface and subsurface microstructure. The SEM (JEOL JSM 5410, Figure 4.3) was used to investigate the samples in this experiment. The samples were prepared by diluting the ZnS particle in ethanol and dispersing in ultrasonic bath for 20 minutes and then droping on the copper stub and drying at room temperature. The gold film was deposited to prevent charging. The specimens were loaded into the sample chamber and used resolution at 15 or 20 kV. Then, the observation was conducted immediately with using image catcher scanner for taking the photo.

4.4.2 Transmission electron microscopy (TEM)

The conventional transmission electron microscope is a key tool for imaging the internal microstructure of ultrathin specimens. In this thesis, the samples were analyzed by using TEM (JEOL JEM-1230) as shown in Figure 4.4. The samples of powder were diluted by ethanol and then dispersed by using ultrasonic bath for 15 minutes for uniform dispersion. One drop of the final solution was poured onto a grid covered with carbon thin film. The specimen was loaded into sample chamber and waiting for the vacuum condition and steady state inside the chamber for 30 minutes.

Figure 4.3 Scanning Electron Microscope (JEOL JSM 5410)

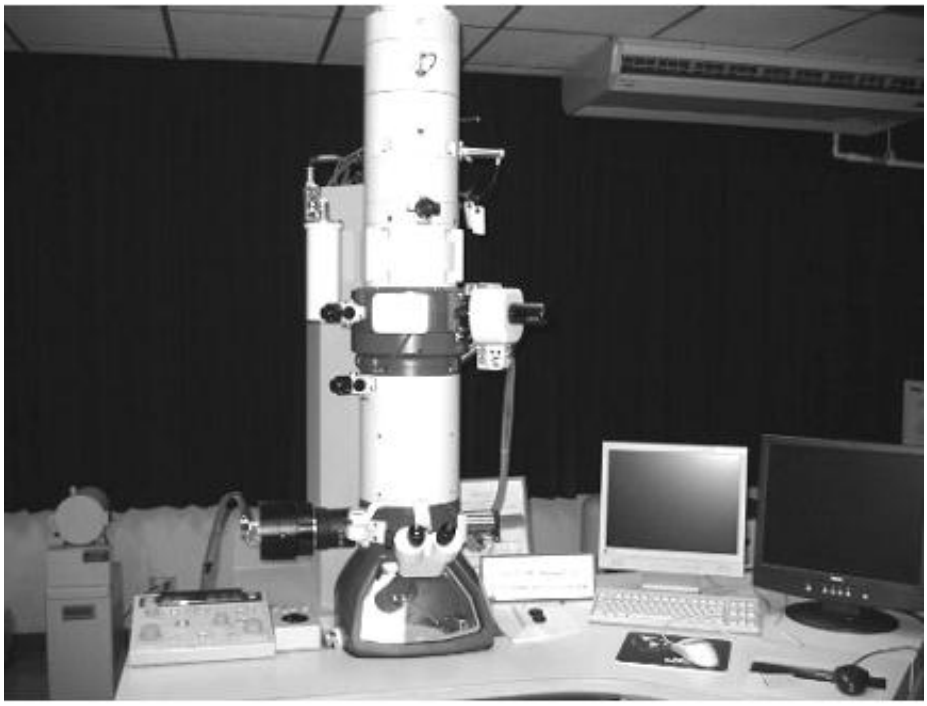

Figure 4.4 Transmission Electron Microscopy (JEOL JEM-1230)

4.4.3 X-ray diffraction (XRD)

X-ray diffraction is of paramount importance in determining the structures of crystals. The application of XRD to nanocrystalline solids, powders, single-crystal thin films or multilayers may be less spectacular. In this experiment, the samples were analyzed by XRD (JEOL JDX-8030) as shown in Figure 4.5 to find their crystalline phase. The ZnS samples were spread on the glass slide and then set in the equipment which provide x-ray beam for the analysis.

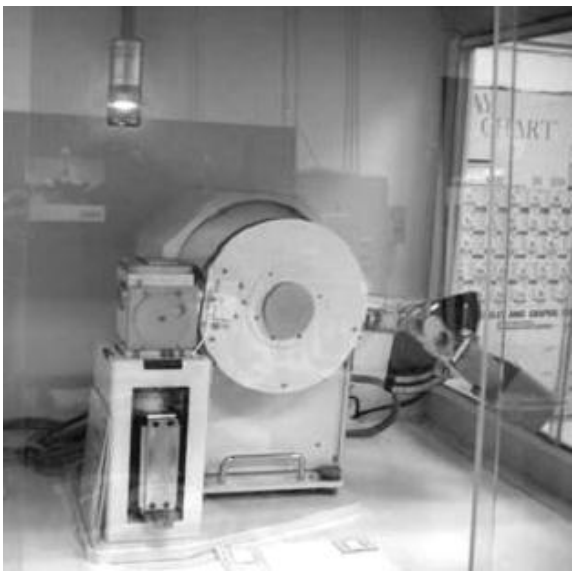

Figure 4.5 X-ray diffraction (JEOL JDX-8030)

4.4.4 Dynamic Light Scattering (DLS)

Dynamic Light Scattering (DLS) is used for particle size analysis. This equipment is based on the measurement of the dispersion of light scattering by particles motion in a static solvent such as ethanol, water or toluene, the measured particle should correspond to hydrodynamic diameter, not the real diameter of complex structures of particles. However, DLS results are expected to give at least the qualitative trend in particle sizes distribution. In this work DLS (ZETA SIZER Nano-ZS) shown in Figure 4.6 were used

for analyzing the resulting nanoparticles. The sample from the final microemulsion was diluted by ethanol. Then, this solution was mixed by homogenizer for 5 minutes and dispersed in ultrasonic bath until ensuring its uniform dispersion, then loaded it to the sample cell for analysis.

Figure 4.6 Dynamic light scattering (ZETA SIZER Nano-ZS)

4.4.5 Photoluminescence (PL)

The photoluminescence (PerkinElmer LS 55) was used to characterize the emission energy ability of the particle or nanocomposite film by using light scattering method. The nanoparticle sample was diluted with ethanol and then filled it into a cuvette sample container for analysis. Otherwise, the nanocomposite film on grass slide can be attached directly to the analyst holder.

4.4.6 Solar cell energy generation

This analysis was a new technique discovered by Energy Research Institute (ERI). This experimental could be achieved by attaching the nanocomposite film on glass slide perpendicular\ to the solar cell as shown in Figure 4.8. The obtained energy was the product of electrical current and voltage detected by a multimeter.

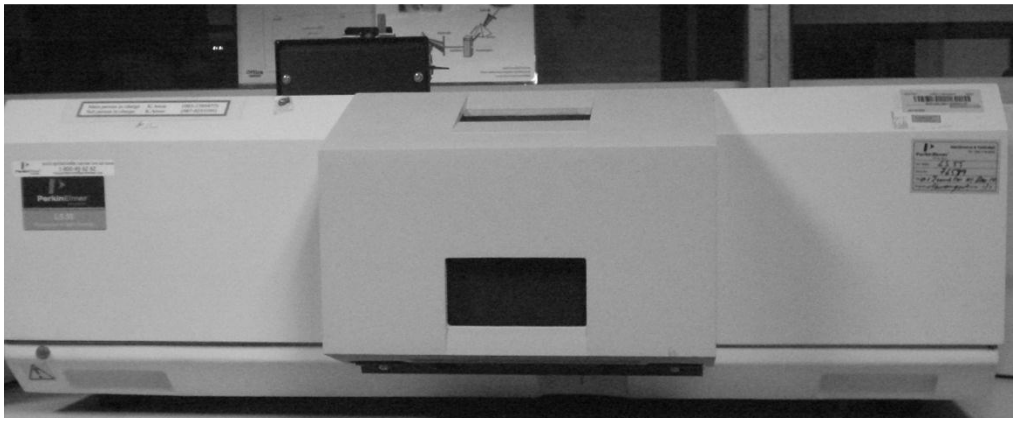

Figure 4.7 Photoluminescence

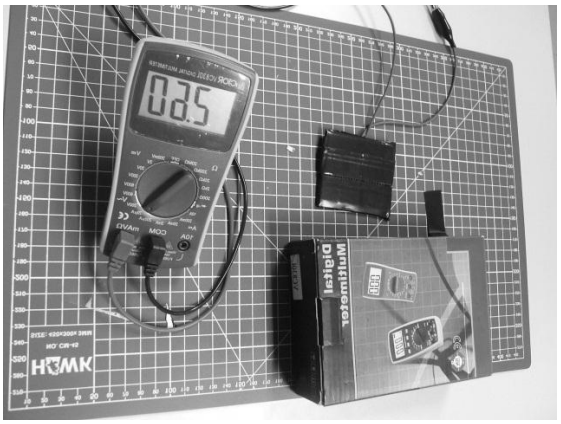

Figure 4.8 solar cell power generation detector

CHAPTER IV

RESULTS AND DISCUSSION

This chapter is divided into two parts. The first section is to investigate of the suspended ZnS in supernatant and the filtrated ZnS nanoparticle. The second is the characterization of PMMA/ZnS composite respected to the compounding conditions and their photoluminescent behavior would be also reported and discussed. This experimental will show characterization of ZnS nanoparticles by microemulsion method. The condition of system has varied precursor concentration and molar ratio of water to surfactant. This work was carried out by precursor concentration (C) of 0.1, 0.2 and 0.5 M and the molar ratio of water to surfactant (W) of 3, 7, and 9. They were named as C01W3, C01W7, C01W9, C02W3, C02W7, C02W9, C05W3, C05W7, and C05W9 as show in Chapter 4 (Table 4.1).

5.1 Investigation of synthesized ZnS nanoparticles

The ZnS characteristics consist of many chemical substances such as oil, surfactant, water and non-reacted reactants should be investigated, although many literatures have done it such variations of parameters. The reasons for the characterizations in ordinarily ways are to investigate the ZnS particles if it is and behaves different from the previous literature that synthesized via micro emulsion method.

The effects of synthesized conditions are characterized by SEM and TEM techniques to investigate their appearance changes of the ZnS particle in both supernatant and filtrated particles. The SEM images of the suspended particle in supernatant and filtrated particle are showed in Figures 5.1-5.2.

The SEM images show that the W ratio increases from C01W3 to C01W9 contribute to increase particles size of ZnS particle both in supernatant and filtrated.

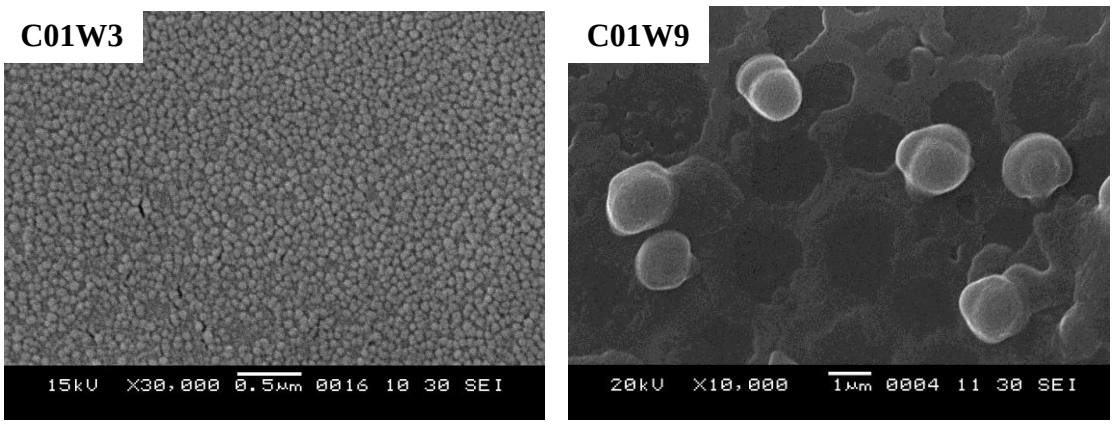

Figure 5.1 SEM images of suspended ZnS particle

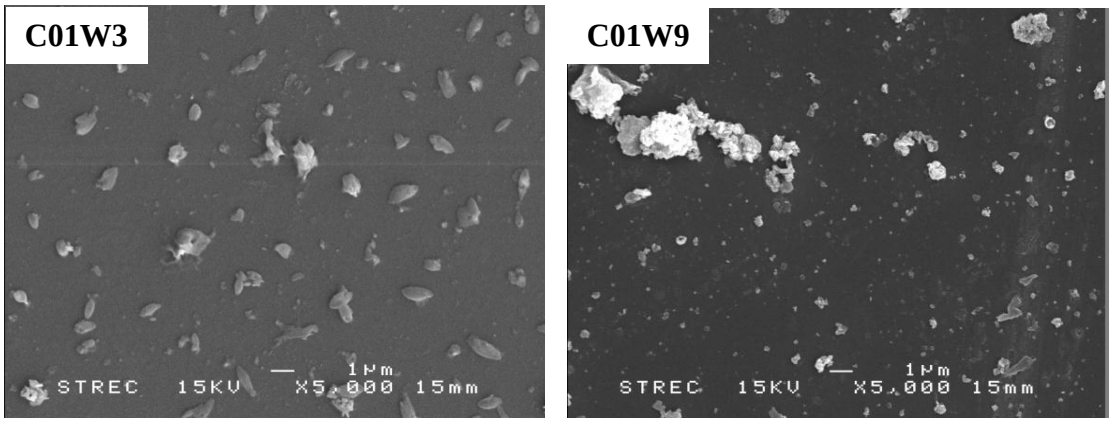

Figure 5.2 SEM images of filtrated ZnS particle

The particles in supernatant seem to be in spheroidal form but the filtrates are in non-shape attributed to agglomeration effect. The SEM images of filtrates are characterized to see the agglomeration as show in Figures 5.3-5.5.

The filtrates of each concentration appear to agglomerate more when W increase which contribute to higher size particle. The agglomeration are in random and cannot be

determined the particle size. In order to determine the ZnS particle size, the suspended particles in supernatant are characterized with TEM images. The TEM images can be further analyzed to determine particle size with particle size distribution. The TEM images and PSD are showed in Figure 5.6-5.8.

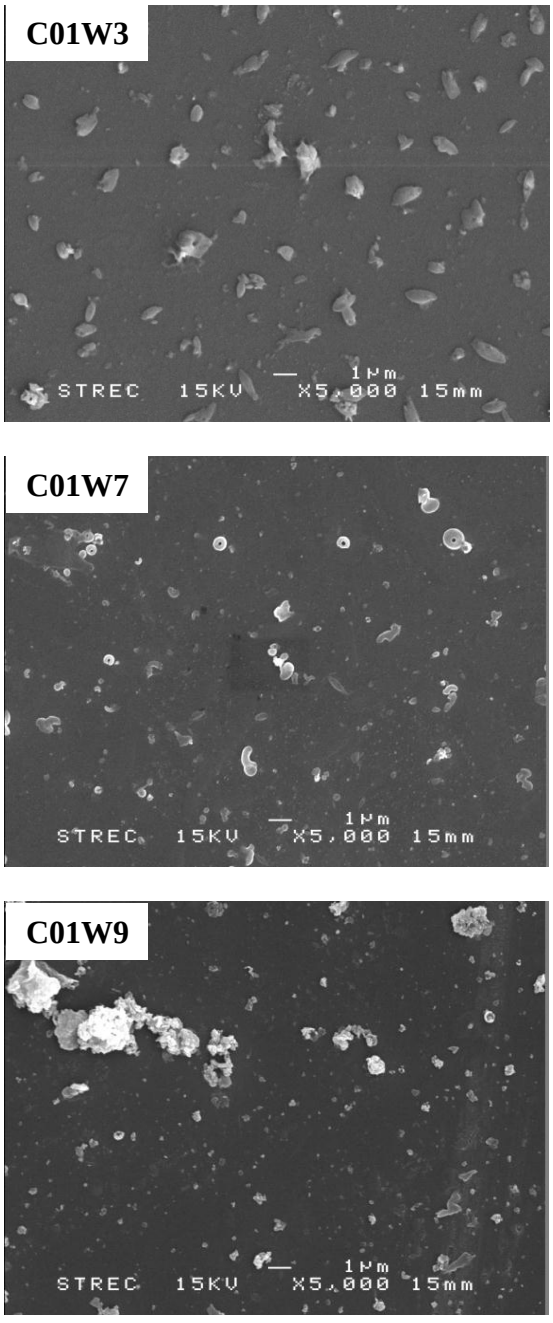

Figure 5.3 SEM images of C01 filtrates

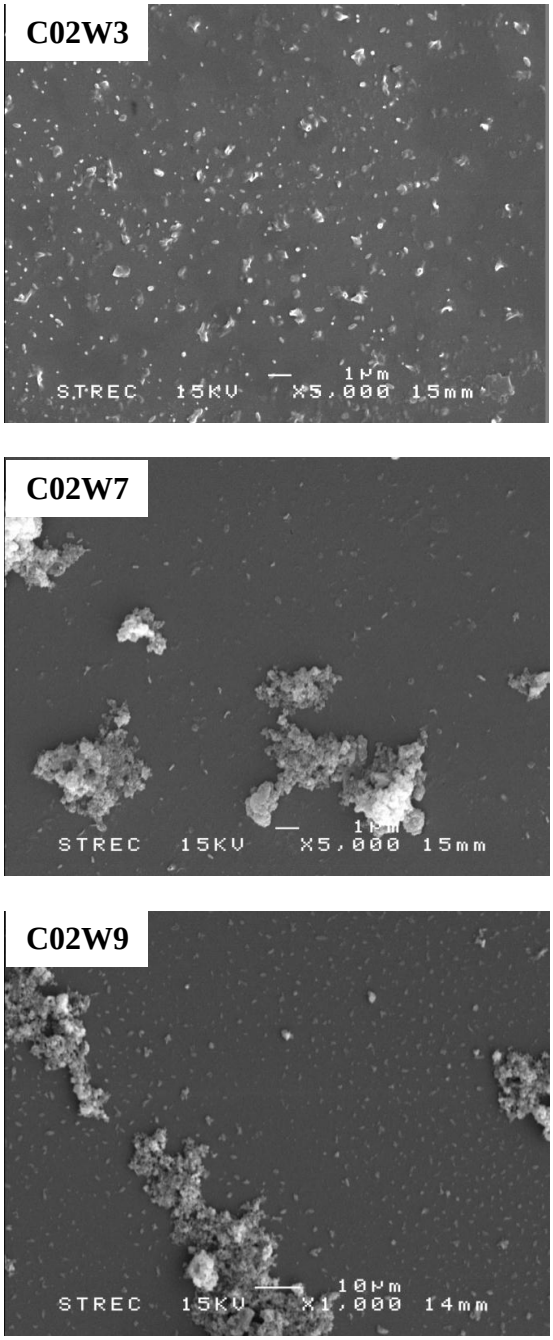

Figure 5.4 SEM images of C02 filtrates

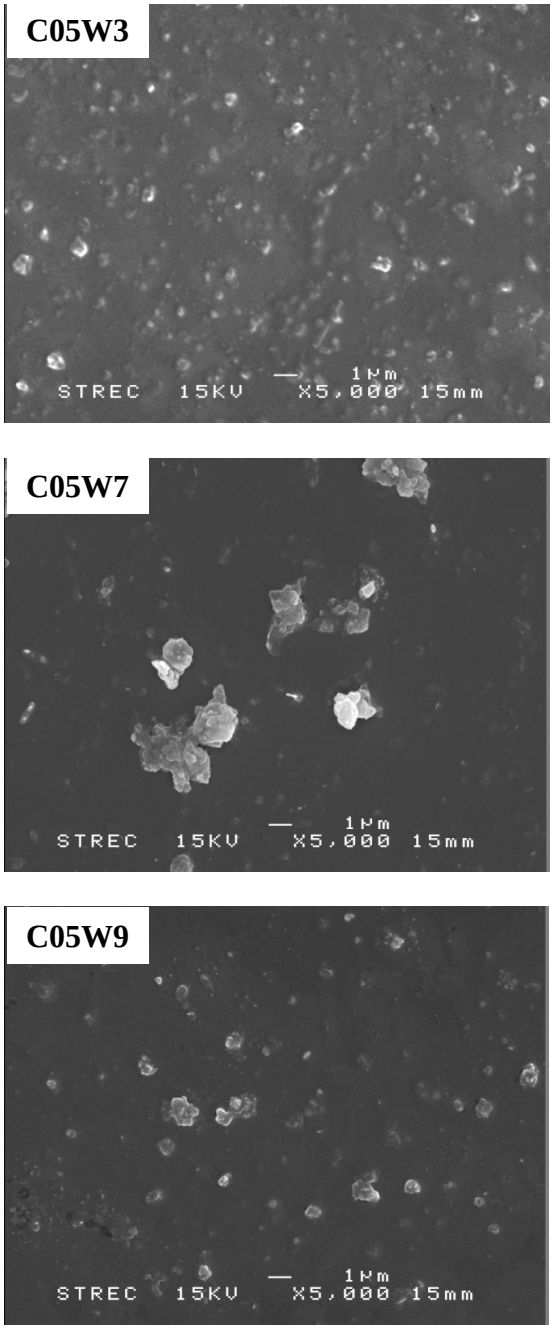

Figure 5.5 SEM images of C05 filtrates

The particle size distribution shows that the average particle size of ZnS in supernatant trend to increase as W increase. These results are the same trend as SEM images. The SEM and TEM results could be concluded that the changing in ZnS particle size varied with water to surfactant ratio, W, may attributed from the different in micelle size. A low W means to a low amount of water. Therefore, the micelle contributes to small because the micelle contains with low amount of water matrix phase. After a small micelle of $ZnSO_4$ reactant interacts with a small micelle of Na_2S reactant, the reactants mass transfers occur to each other and form the ZnS particle in each small micelle. This relevant model was also mentioned and proposed by Ashok et al. [86]. The possible model of ZnS formation varied with W was showed in Figure 5.9.

Although the SEM and TEM can reveal the variation of particle size formation, the ZnS particle should be investigate further to determine the significant size-controlling parameters and their dependencies. Various techniques should be carried on them.

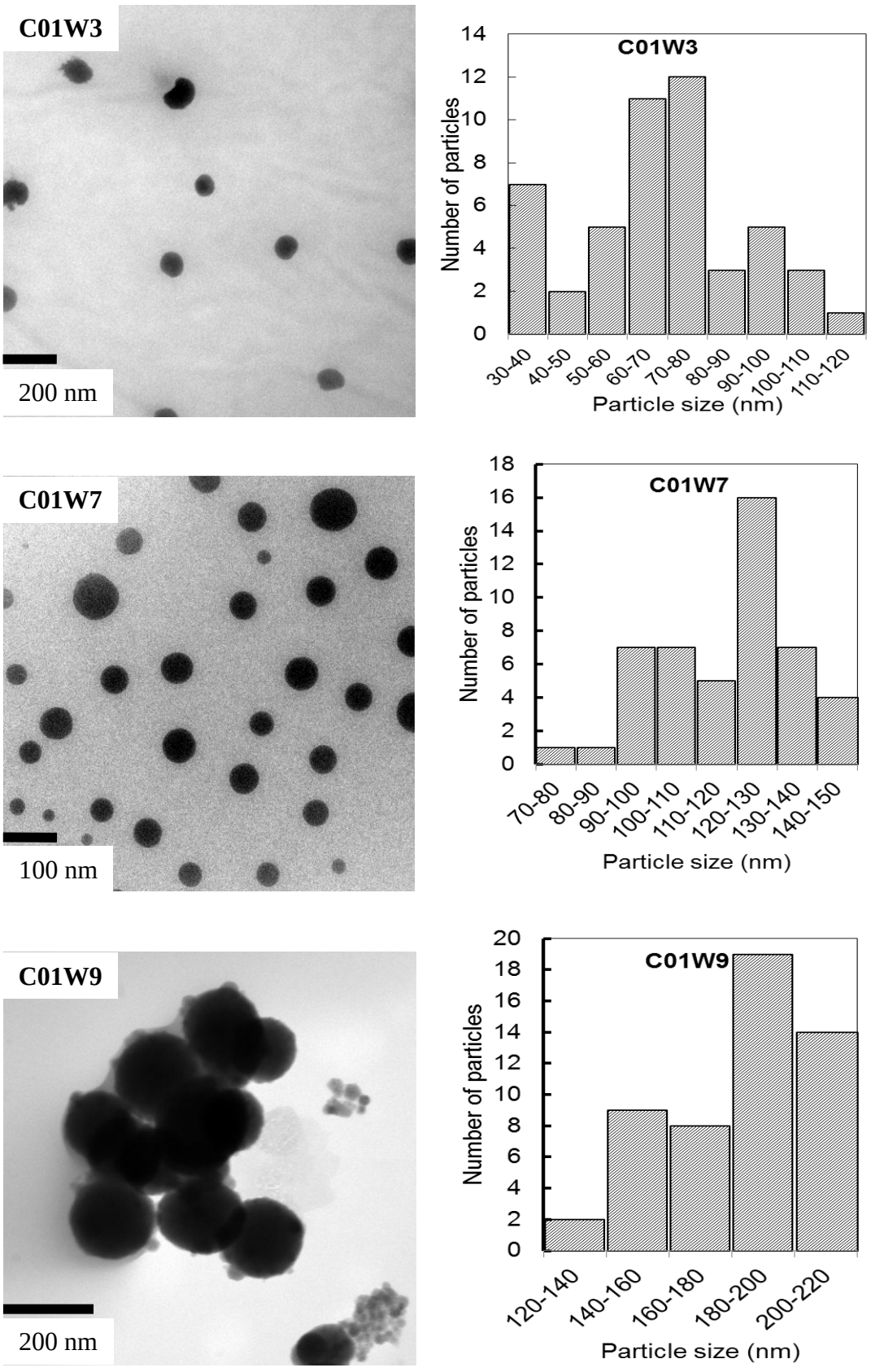

Figure 5.6 TEM images of C01 suspended particle ZnS nanoparticle and PSD

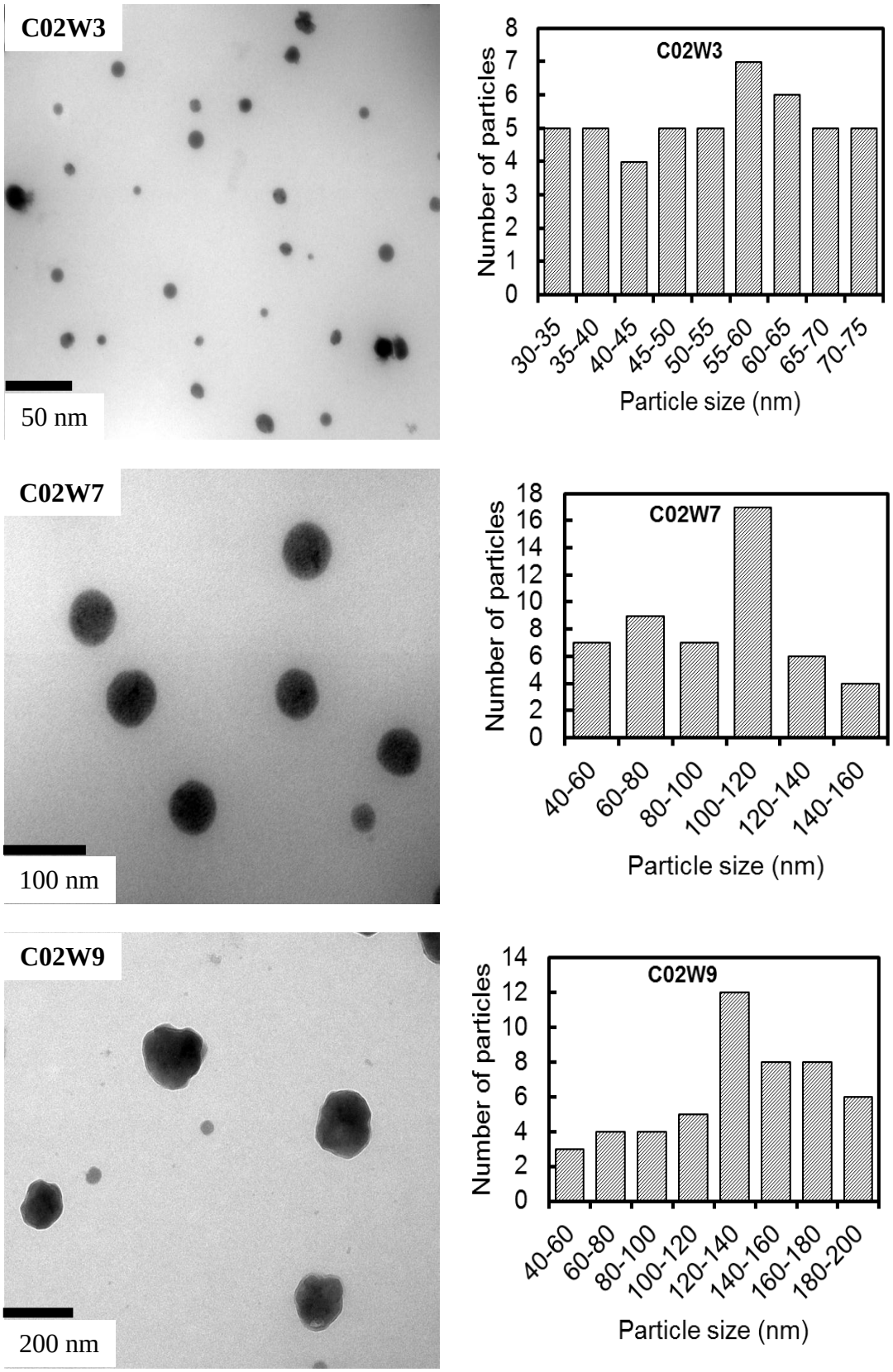

Figure 5.7 TEM images of C02 suspended particle ZnS nanoparticle and PSD

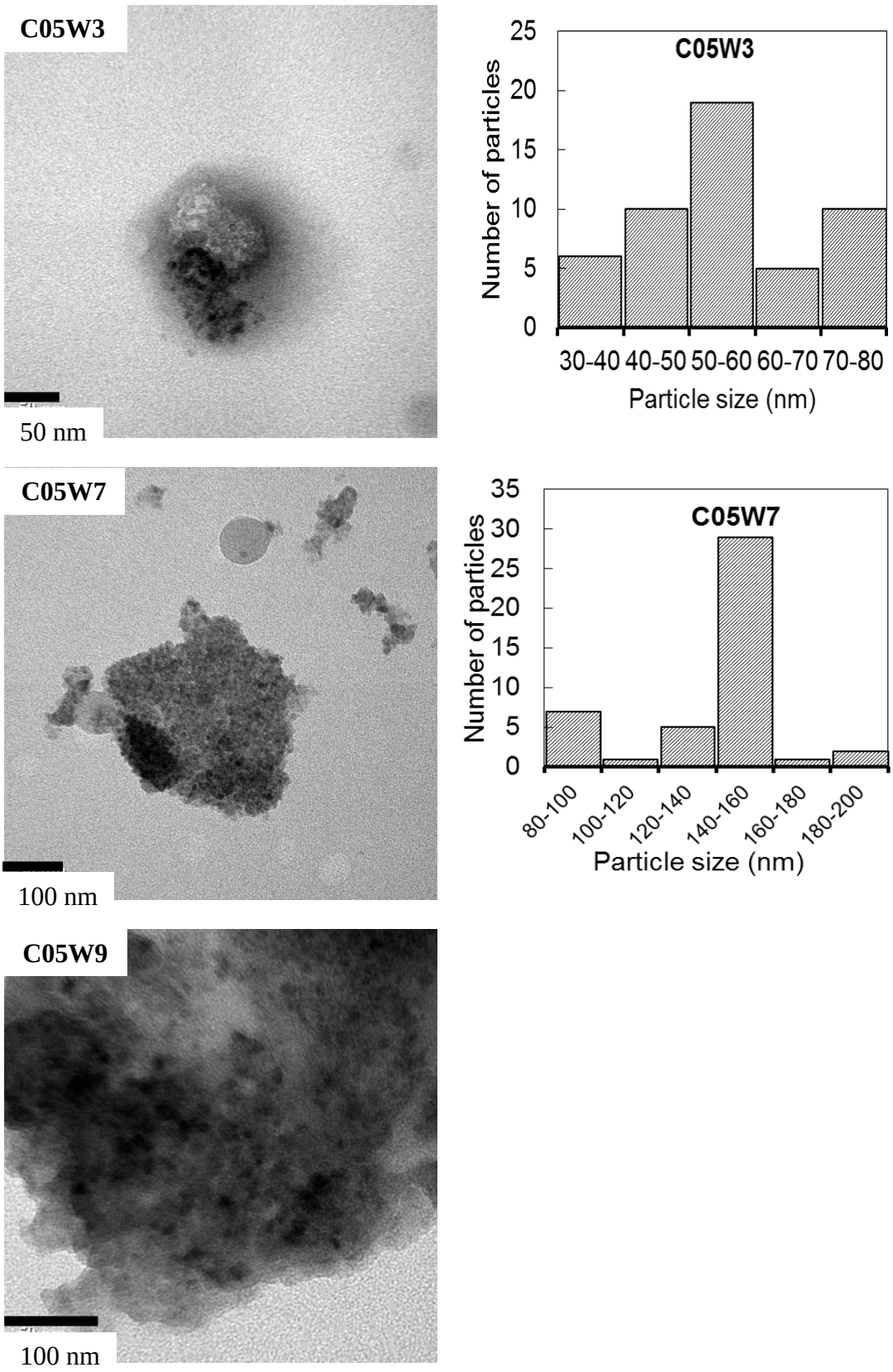

Figure 5.8 TEM images of C05 suspended particle ZnS nanoparticle and PSD

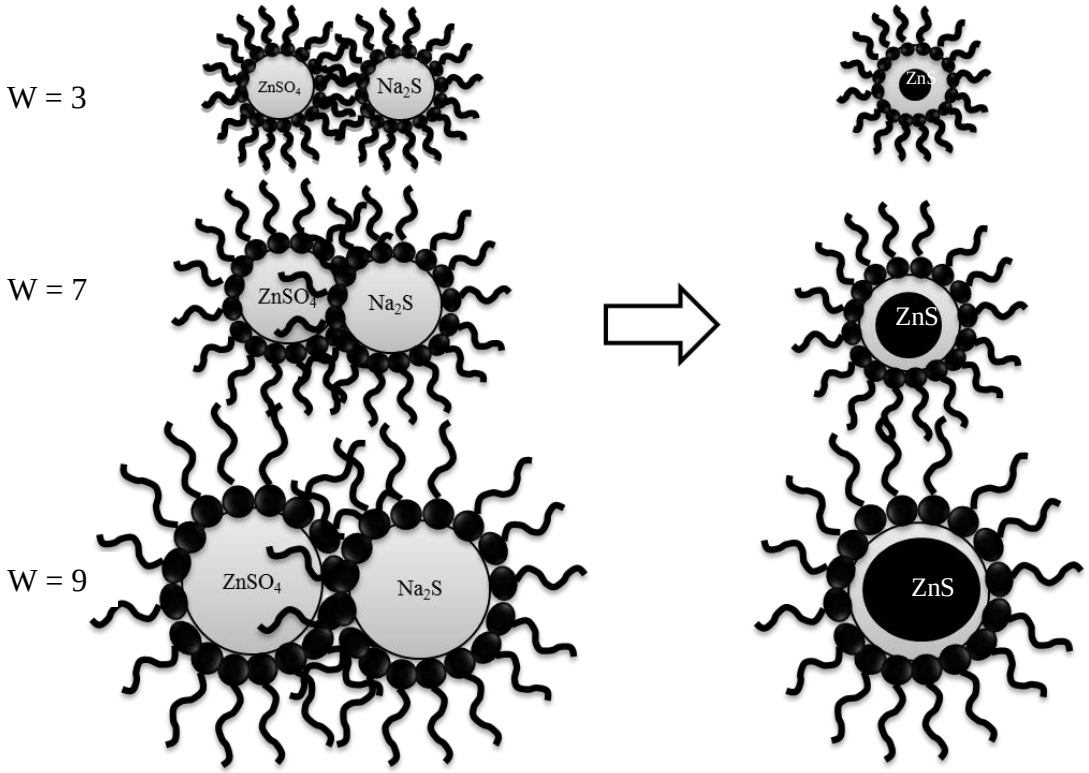

Figure 5.9 Model of ZnS formations on the variation of W

Crystallinity is one of the physical solid properties which can be observed by selected area electron diffraction (SAED). The SAED images are showed in Figure 5.10

The electron diffractions exhibit rather clearly that a low W and low C condition gives a low crystallinity, otherwise, a high W and high C condition gives a high crystallinity as a comparison between C01W3 and C05W9.

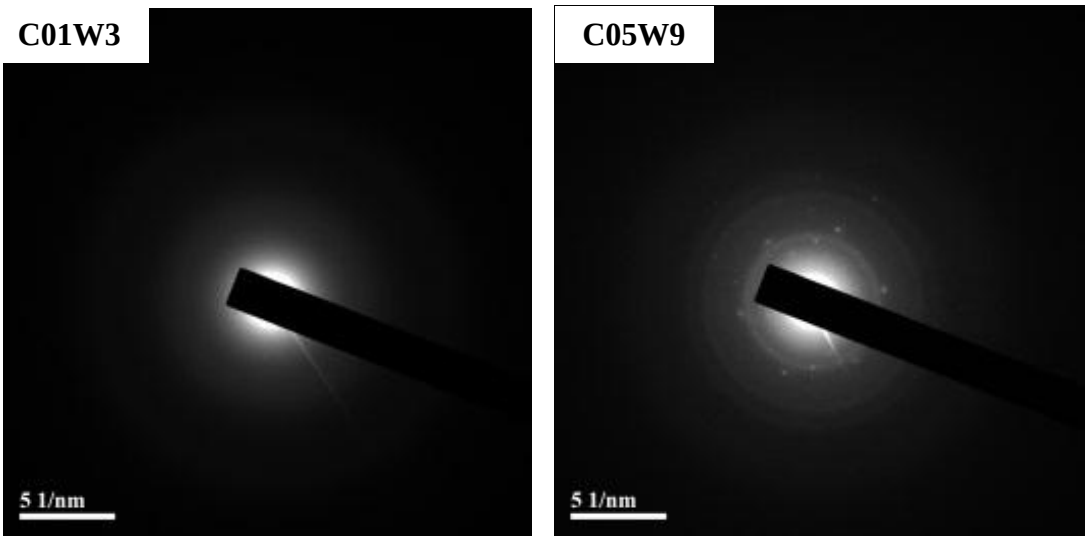

Figure 5.10 SAED images of C01W3 and C05W9 ZnS particle

XRD is a condition equipment to investigate the crystallinity of solid. The XRD carries on each filtrated ZnS particle synthesized with different condition. The XRD spectra are showed in Figure 5.11.

The XRD spectra of each ZnS particle exhibit multiple peaks on a plane of [111], [220], and [311] which represented to the ZnS nanoparticles in cubic crystal form without any contaminates. The intensity of C05W9 shows the highest amplitude which indicates to highest crystallinity and this result consistent with the SAED results. Furthermore, the particle size is able to calculate based on XRD data according to the following Debye–Scherrer formula [82].

$$L = \frac{0.9\lambda}{\beta \cos\theta} \qquad (5\text{-}1)$$

Where *L* is the coherence length, B is the full width at half maximum (FWHM) of the diffraction peak, λ is the wavelength of the X-ray radiation, and θ is the Bragg angle of the diffraction peak. The relation between *L* and *D*, the diameter of the crystallite, is given by $L=3D/4$, assuming the particles is in spherical shape. The Table 5.1 shows the dependent of average sizes of ZnS nanoparticles and synthesis conditions. The average crystallite size of ZnS nanoparticle trends to increase as C or W increase. The C01W3 particle is the smallest crystallite sizes while the C05W9 particle was the highest size. The results could be explained that both of the parameter C and W effected to the crystallite size.

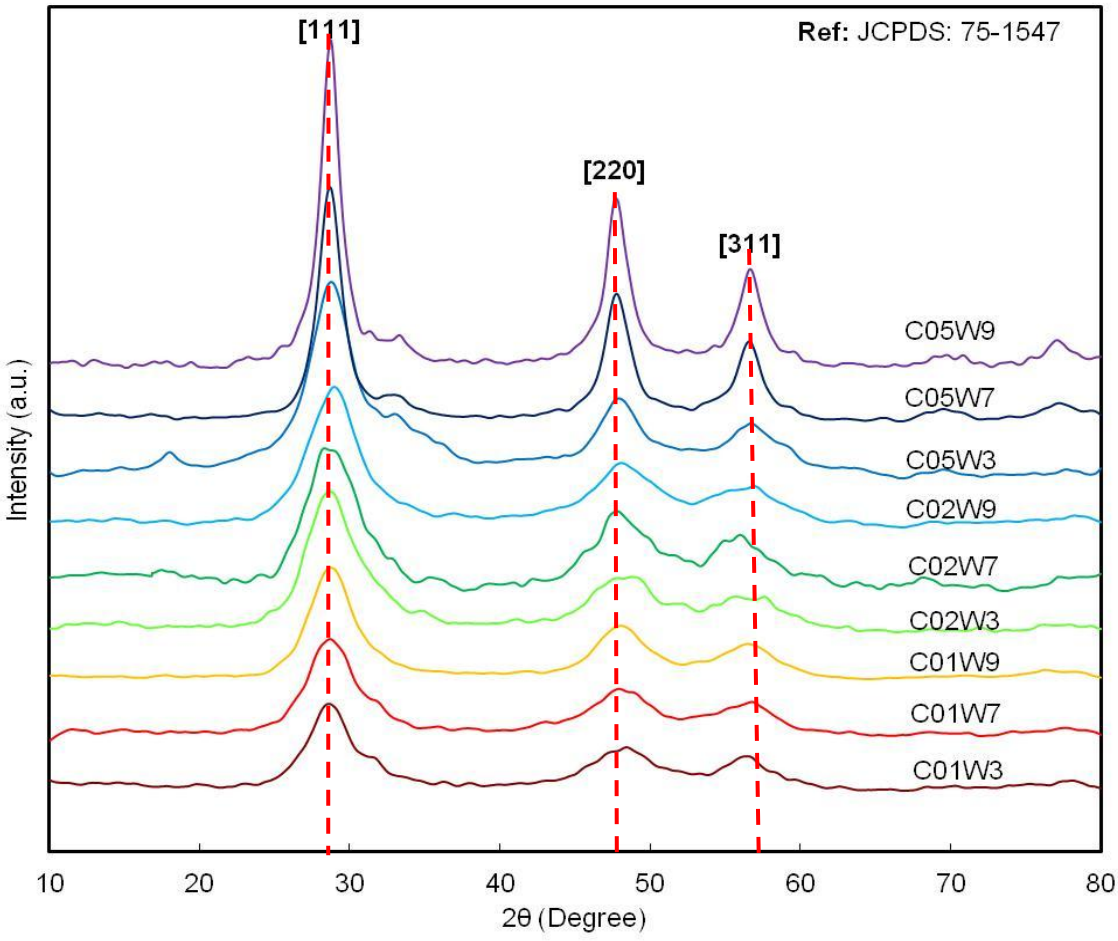

Figure 5.11 XRD spectra of filtrated ZnS particle

Table 5.1 Average crystallite size of ZnS nanoparticles calculated from XRD data

C01W3	C01W7	C01W9	C02W3	C02W7	C02W9	C05W3	C05W7	C05W9
2.3 nm	2.4 nm	2.8 nm	2.3 nm	2.4 nm	2.3 nm	2.3 nm	5.3 nm	6 nm

The precise data calculated from XRD which reveal that the crystallite size increases as the concentration and water increase. The model on Figure 5.9 should be considered to be co-explained the phenomena in the synthesis of ZnS particle via microemulsion method. As mentions on the effect of W, amount of water is directly variation with the micelle size. When the amount of water is low, the ZnS particle cannot be produced larger than this criterion. This explanation is the answer for the same crystallite size compared between C01W3 and C05W3 which have low amount of water but different in concentration. In the other hand, the limitation can be reduced by increasing water amount and then the ZnS particle can grow freely without any criteria that why this work shows the different crystallite size between C01W9 and C05W9.

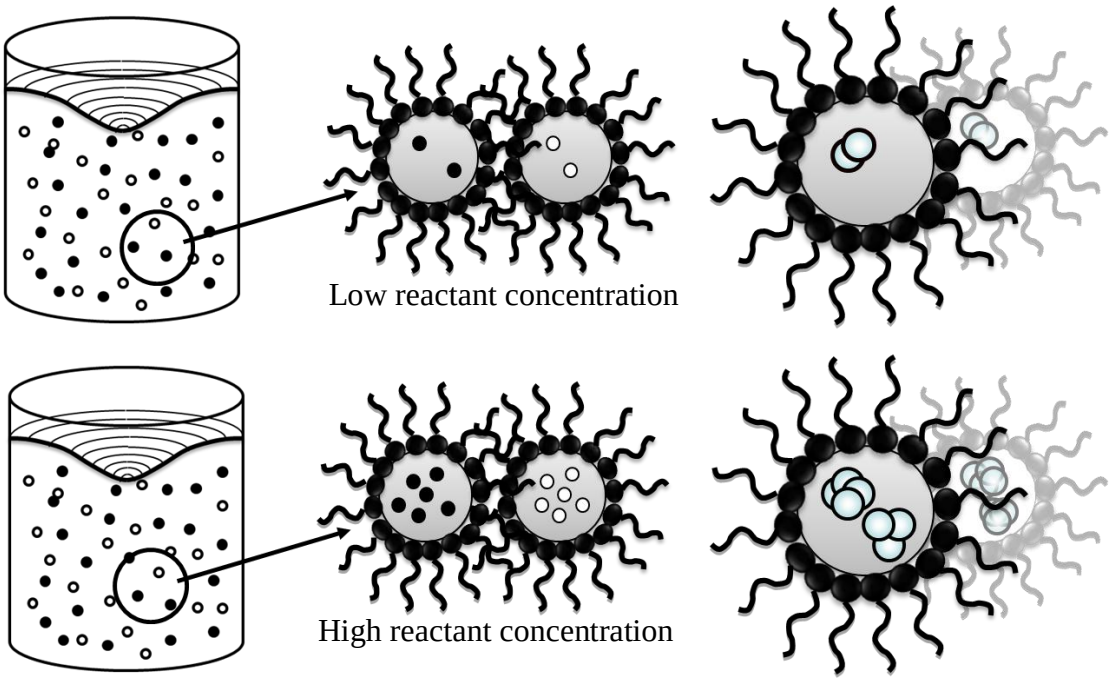

Figure 5.12 Formation of ZnS crystal of various precursor concentrations

The filtrated ZnS particle is considered to be utilized as a dopant comprising with PMMA. For utilizing, the ZnS particle should be found out the luminescence ability firstly. In order to use the photoluminescence, the excitation wavelength must be known to active the emission spectra in high magnitude. Many literatures have found on this data. The excitation wavelength located on 280 nm and the emission located in a range between 350-500 nm [81-83]. The photoluminescence spectra are showed in Figure 5.13.

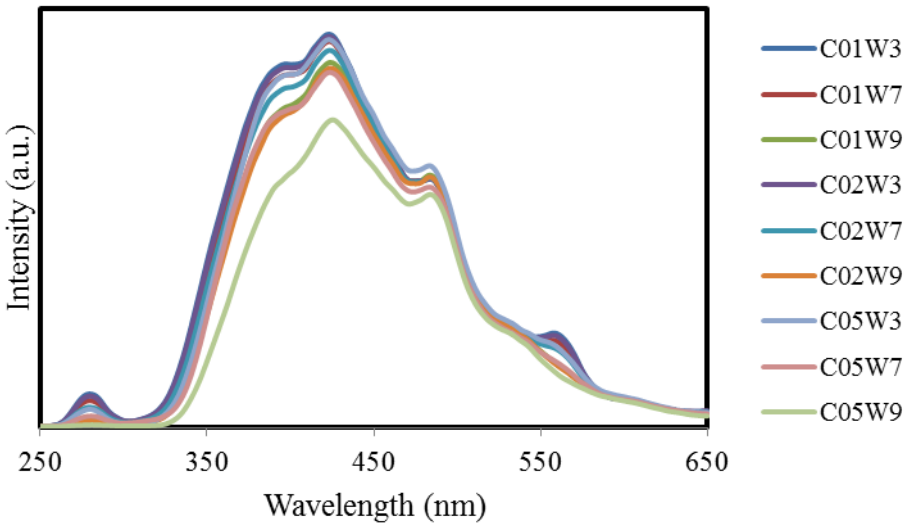

Figure 5.13 Photoluminescence spectra of filtrated ZnS particle

The spectra show different intensities. The largest crystallite size particle (C05W9) exhibits the lowest intensity which means to have the lowest luminescence ability. Otherwise, the small size particles exhibit the high luminescence intensity. Based on this result, the ZnS particle could be utilized as an improvement of PMMA in order to give better luminescence ability.

5.2 Investigation of ZnS/PMMA nanocomposite

The ZnS/PMMA nanocomposite materials are produced in two types; 1) PMMA

film and 2) PMMA commercial sheet. They are investigated on the particle distribution on materials and the improvement of luminescence abilities after comprised with ZnS nanoparticle and their power generation ability when they are combined with solar cell as the solar concentrator.

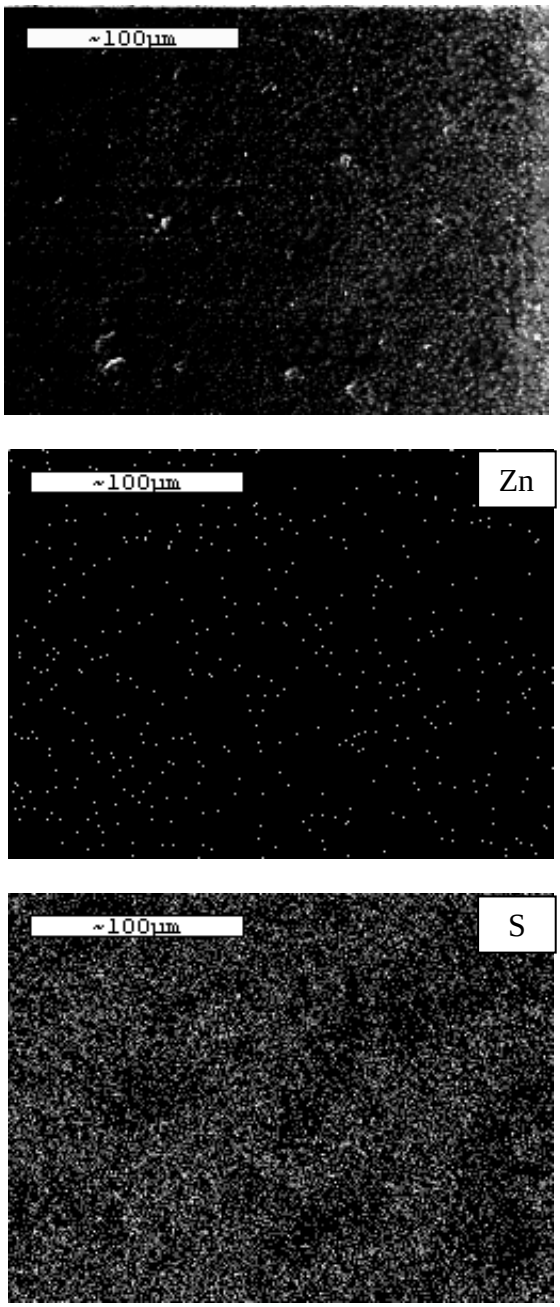

Figure 5.14 SEM-EDX of C01W9 ZnS/PMMA composite film

The distributions on the materials are investigated by SEM-EDX which the results show that the distribution is dispersed well on both film type and commercial sheet type as show in Figure 5.14-5.17.

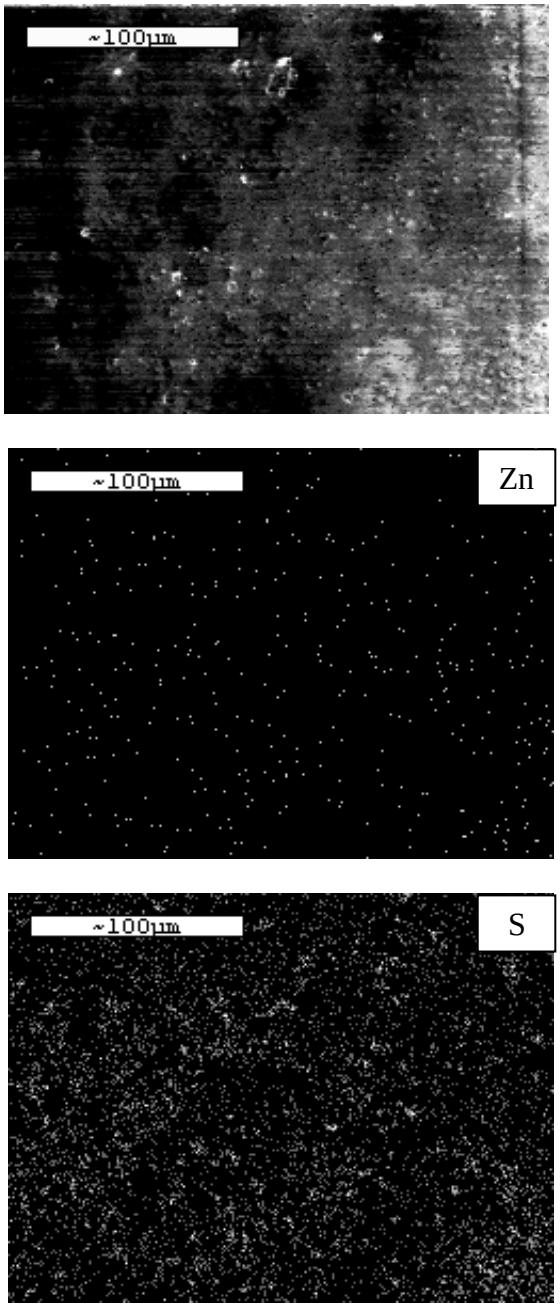

Figure 5.15 SEM-EDX of C05W9 ZnS/PMMA composite film

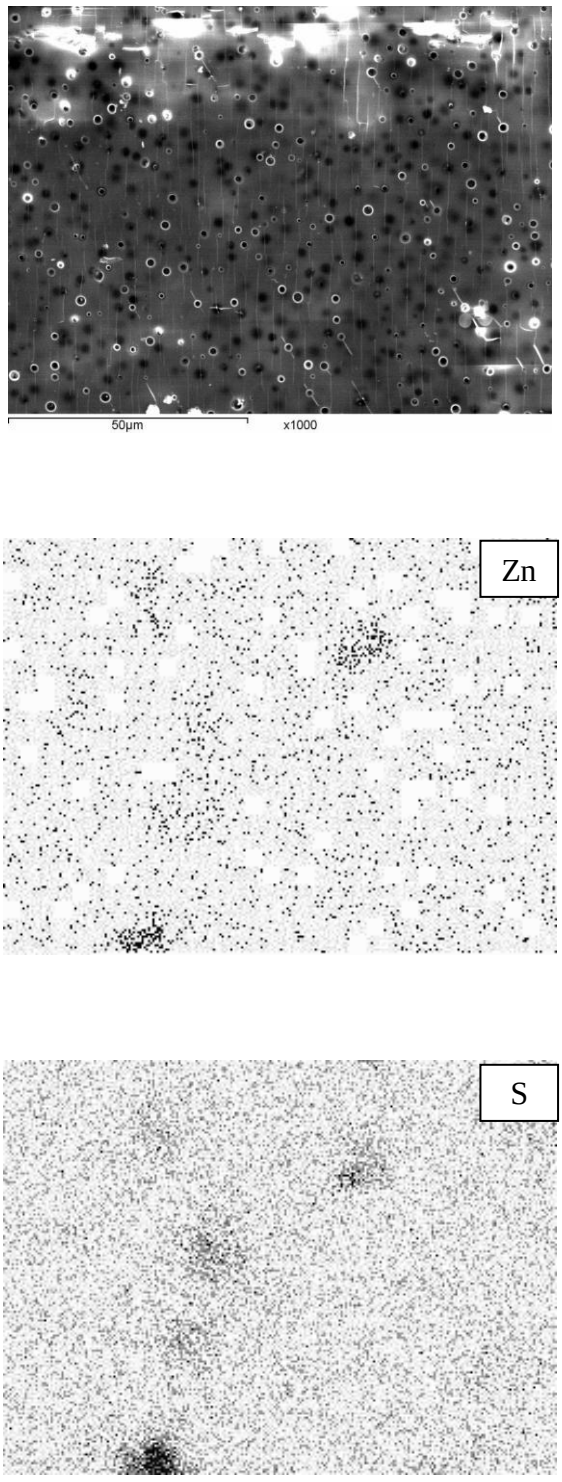

Figure 5.16 SEM-EDX of C01W3 ZnS/PMMA composite sheet

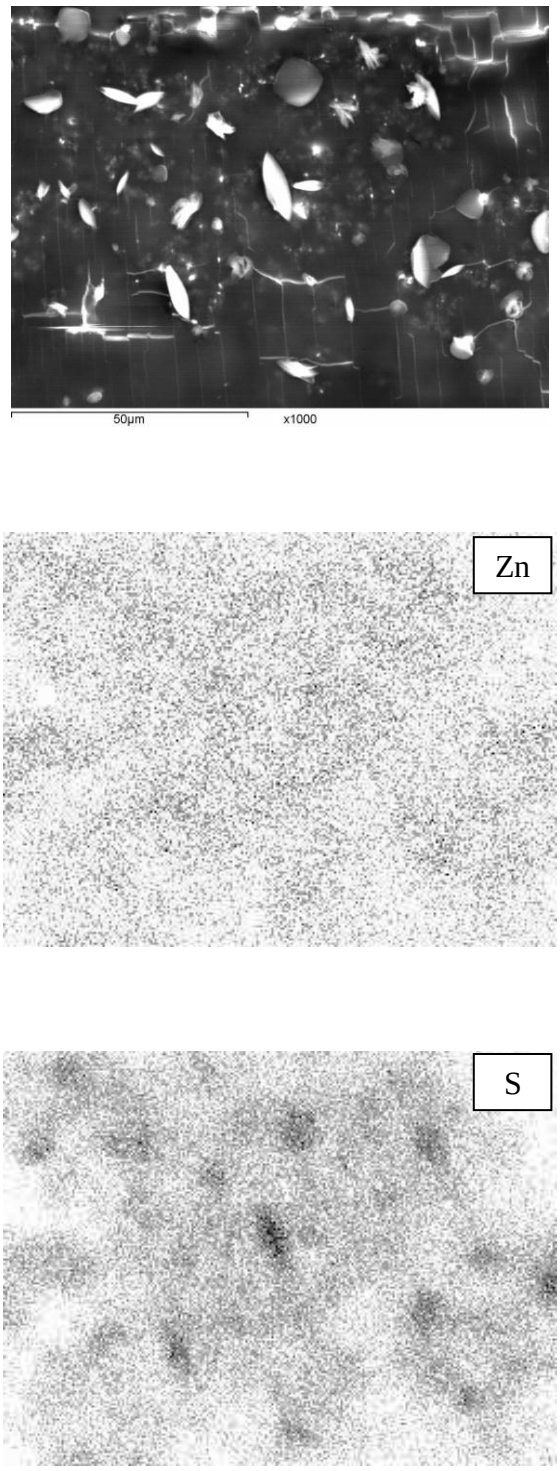

Figure 5.17 SEM-EDX of C01W9 ZnS/PMMA composite sheet

The photoluminescence spectra of ZnS/PMMA films are showed in Figure 5.18. The photoluminescence spectra of ZnS/PMMA nanocomposite film reveal the same trend as filtrates, which the smallest crystallite size particle has the highest luminescence energy and vice versa. The amounts of ZnS dopant also affect to the luminescence abilities, in addition, the higher amounts of dopant give the higher luminescence.

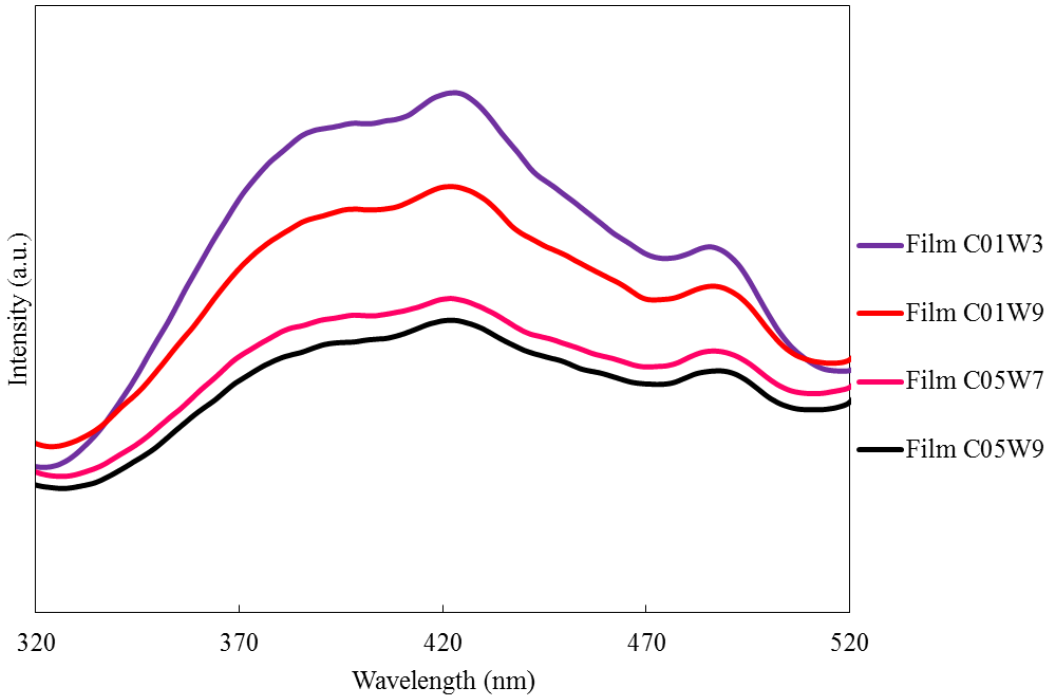

Figure 5.18 Photoluminescence of ZnS/PMMA film

The power generation abilities when the composite film connected to solar cell are also investigated. The power generation abilities are showed in Figure 5.20-5.21. The power generation shows that the solar cell has more power generation after using ZnS/PMMA film compared to pure PMMA film and the small crystallite size and the many amount of particle exhibit a high power generation which consistent with PL results.

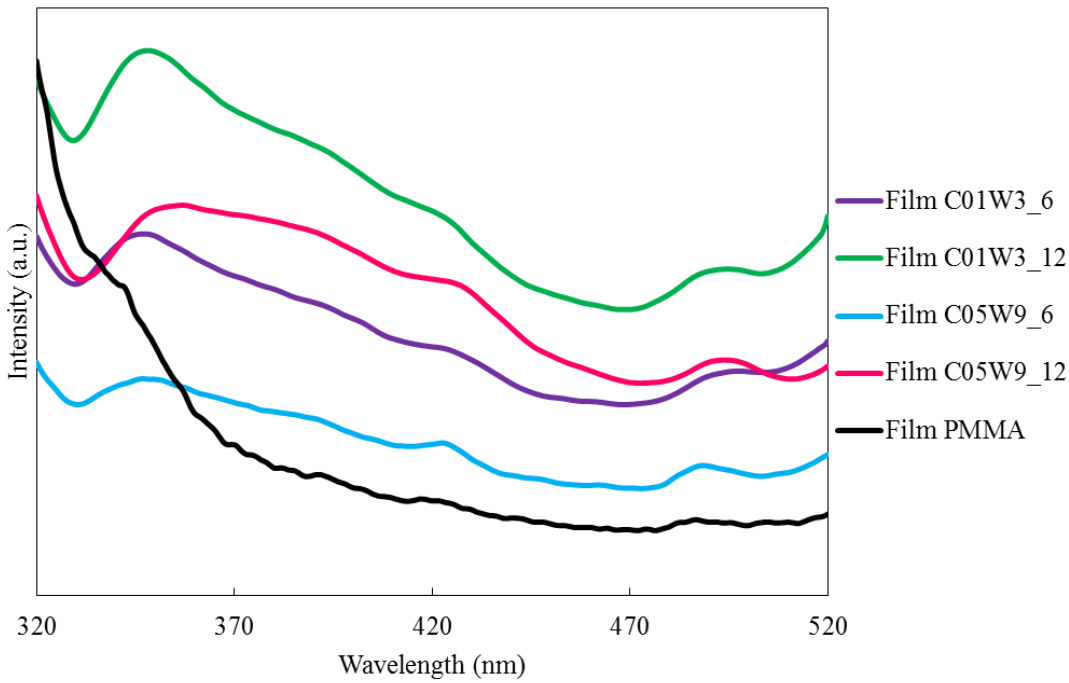

Figure 5.19 Photoluminescence of ZnS/PMMA films with various amounts of ZnS

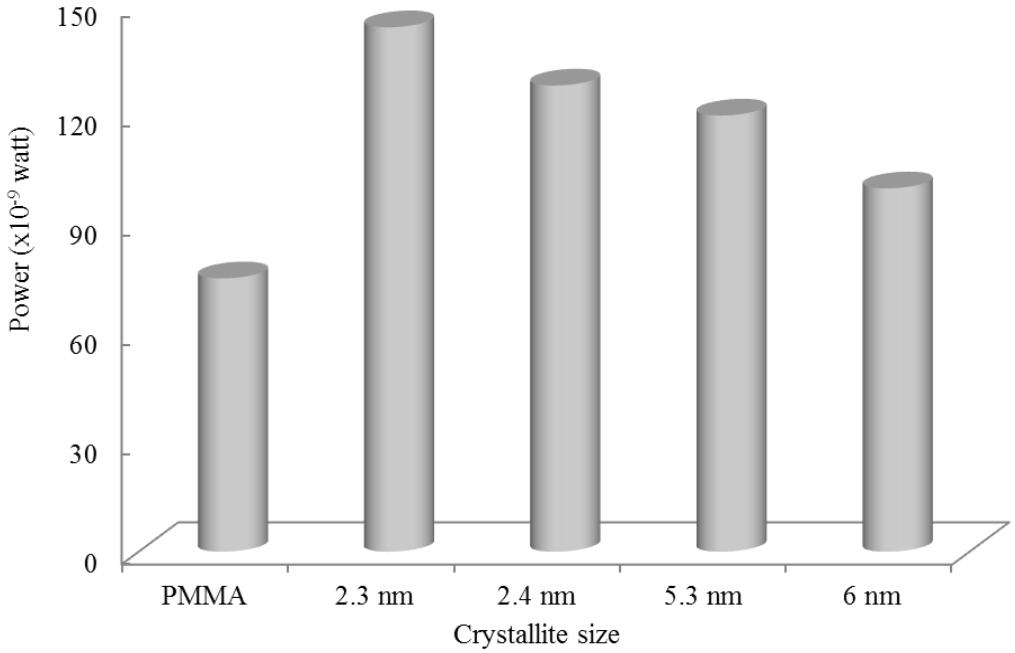

Figure 5.20 Power generation of using ZnS/PMMA film as solar concentrator

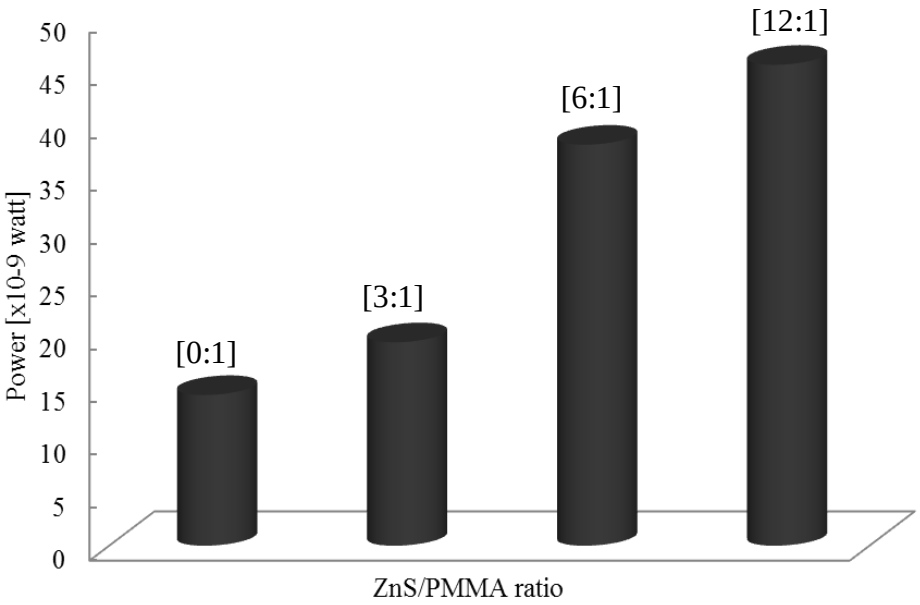

Figure 5.21 Power generation of various C01W3ZnS/PMMA ratios

The ZnS/PMMA commercial sheet type is also investigated on the same techniques as the films. The composite sheet photo luminescence and power generation ability are showed in Figure 5.22-5.23.

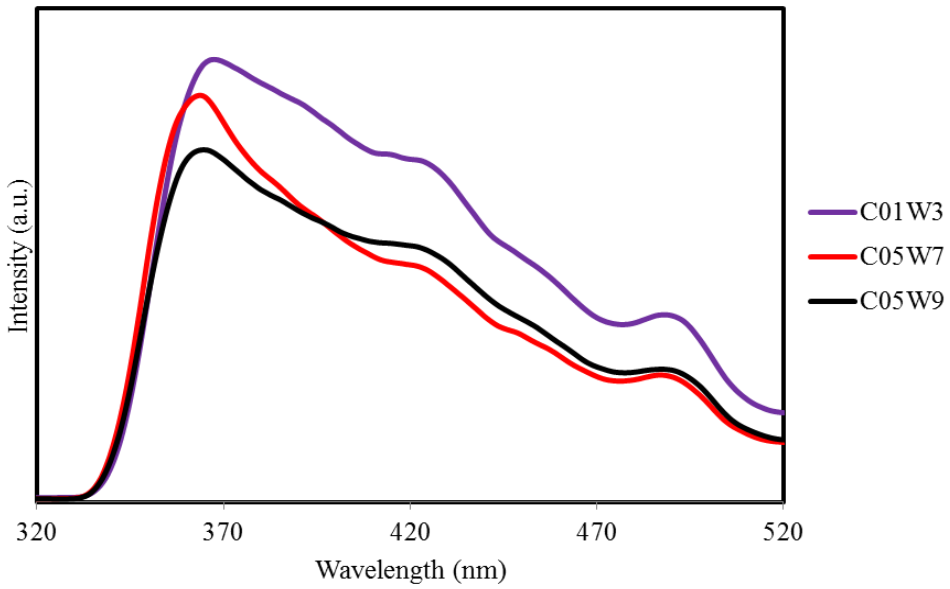

Figure 5.22 Photoluminescence of ZnS/PMMA sheet

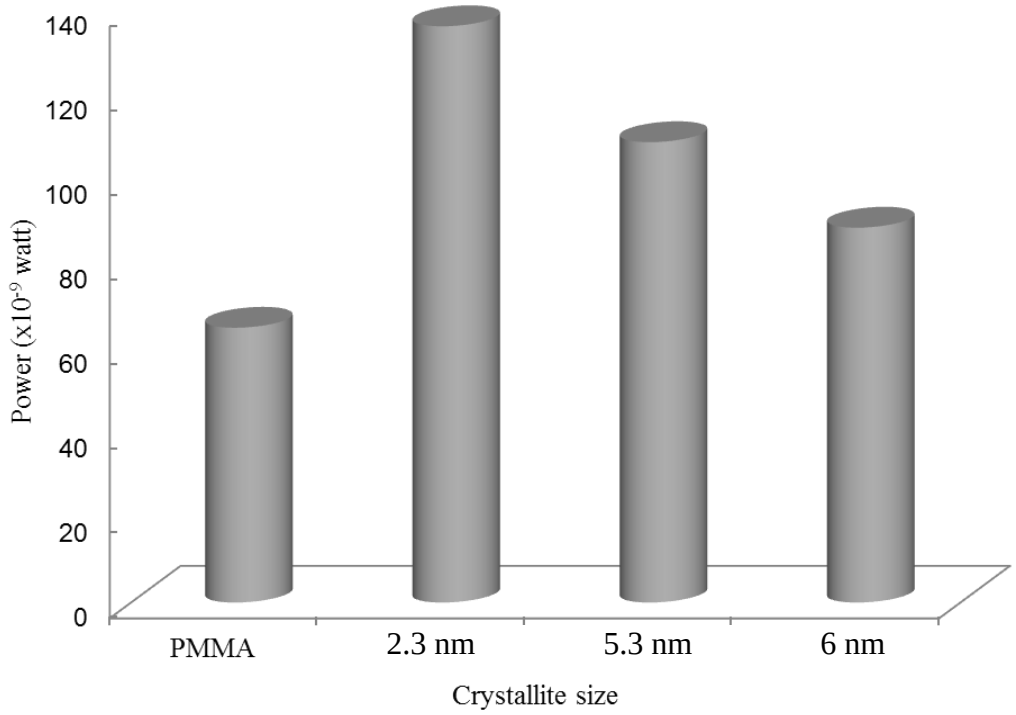

Figure 5.23 Power generation of using ZnS/PMMA sheet as solar concentrator

The addition of ZnS nanoparticle produced via microemulsion method was advantage to improve the emission ability of PMMA which cannot emit luminescence energy in visible range of 350-500 as the ZnS can do. Although the agglomeration cannot be overcome, it did not affect significantly to the trend of luminescence energy. The ZnS/PMMA nanocomposites are also investigated and revealed to approach the application prototype. It also showed that the small crystallite site exhibited the highest power generation as same as the photoluminescence results.

CHAPTER VI

CONCLUSIONS AND RECOMMENDATIONS

6.1 Conclusions

The microemulsion using reverse micelle method can produce a small ZnS nanoparticle. The particle size of the ZnS may be not only the significant parameter affecting the photoluminescence behavior. This work reveals that the emission properties depend on the crystallite size which depends on the synthesized condition. It was believed that the water to surfactant molar ratio (W) was believed that it is the significant parameter to control the size of the particle. However, this work has revealed that there are not only the W parameters affecting the size but also the reactant concentration in the mixture solution. As described in proposed model, the reactant concentration increased, the opportunity to from the crystallite size was high.

The crystallite size of the ZnS nanoparticle produced from a low W and a low C condition is small. This small crystallite size and the high amount of ZnS give the high photoluminescence ability and, therefore, gives the high electrical energy production of the solar cell as the result of using a small crystallite size composed with PMMA utilized as a solar collector.

6.2 Recommendations

This research should be studied further on;

1. The effect of dispersion of the particle on the emission and how to handle it to be well dispersed particle

2. How to increase yield of the synthesized nanoparticle
3. The possibility to use the ZnS nanoparticle on the commercial industry
4. The more suitable chemicals substitute to the cyclohexane, octanol and MMA which are toxic and smell chemicals.

REFERENCES

[1] Van Sark, W.G., et al. Luminescent Solar Concentrators: A Review of Recent Results, J. Opt. 2008:21773-21792.

[2] Grieve, K., Mulvaney, P., and Grieser, F. Current, Synthesis and electronic properties of semiconductor nanoparticles/quantum dots, Opin.Colloid Interface Sci, 2000:168-172.

[3] Wikipedia. Quantum dot [online]. 2012. Available from : http://en.wikipedia.org/wiki/Quantum_dot. [2012, April].

[4] Huang, J., Xia, C., Cao, L., and Zeng, X. Facile microwave hydrothermal synthesis of zinc oxide one-dimentional nanostructure with three-dimentional morphology, Mater. Sci. Eng. 2008:187-193.

[5] Xu ,X. and Li, X. Formation of zinc sulfide nanorods and nanoparticles in ternary W/O microemulsions, J. Colloid Interface Sci, 2003: 275-281.

[6] Shen, X., Du, Y., Yang, P and Jiang, L. Morphology control of the fabricated gold nanostuctures in W/O microemulsion under microwave irradiation, J. Phys. Chem. Solids, 2005:1628-1634.

[7] Li, Y., He, X. and Cao, M. Micro-emulsion-assisted synthesis of ZnS nanospheres and their photocatalytic activity, Mater. Res. Bull., 2007: 3100-311.

[8] Wang ,L., et al. properties and simultaneous synthesis of ZnS and ZnO nanoparticles via one reverse micellar system, Colloids Surf., 2010: 205–209.

[9] Zeng, H.Z., Qiang, K., Yuan, Q., and Li.,W. Z. A new way to synthesize ZnS nanoparticles, Chin. Chem. Lett., 2007:483–486.

[10] Xu , Li. Synthesis and characterization of shaped ZnS nanocrystals in water in oil microemulsions,.Mater. Res. Bull., 2003: 4396-4399.

[11] Lv, R. and Cao, C. Synthesis and characterization of ZnS nanowires by AOT micelle-template inducing reaction, Mater. Res. Bull., 2004:1517-152.

[12] Thawatchai Charinpanitkul,and Amonsak Chanakul. Effects of cosurfactant on ZnS nanoparticle synthesis in microemulsion, Sci. Technol. Adv. Mater., 2005: 266-271.

[13] Arai, K., et al. Photoluminescence and cathodoluminescence studies of ZnSe quantum structures embedded in ZnS. J. Cryst. Growth., 184/185 (1998): 254-258.

[14] Franco, D., et al. Enhancement of PMMA nonlinear optical properties by means of a quinoid molecule. Opt. Mater., 2004: 661–665.

[15] Li, Y., Ding, Y., Zhang, Y., and Qian. Y. Photophysical properties of ZnS quantum dots. J. Phys. Chem. Solids., 1999: 13–15.

[16] Rowan, G., and Norton, B. Quantum dot solar concentrator: Device optimization using Spectroscopic Techniques. Sol. Energy., 2007: 540–547.

[17] Qian, L. , Zhang, T., Teng, F. , Xu, Z., and Quan, S. Luminescent properties and excitation mechanism of ZnS quantum dots embedded in ZnS Matrix. Mater. Chem. Phys., 2006: 337–339.

[18] Gallagher, S.J., Norton, B., and Eames, P.C. Quantum dot solar concentrators:Electrical conversion efficiencies and comparative concentrating factors of fabricated devices. Sol. Energy, 2007: 813–821.

[19] Geo, L., Chen, S., and Chen, L. Controllable synthesis of ZnS/PMMA nanocomposite hybrids generated from functionalized ZnS quantum dots

nanocrystals. Colloid. Polym. Sci., 2007: 1593–1600.

[20] Philips, J.C., and Lucovsky, G. Crystal Structures. Bonds and bands in semiconductors. pp 1-25. NY: Momentum Press, 2009.

[21] Colorado University. Principle of semiconductor device [Online]. 2011. Available from: http://ecee.colorado.edu/~bart/book/book/chapter2/ch2_3.htm#fig2_3_8 [2012, April]

[22] Philips, J.C., and Lucovsky, G. Crystalline semiconductor interfaces. Bonds and bands in semiconductors. pp 280-291. NY: Momentum Press, 2009.

[23] Nattapun Suppaga. Physical dimensional limitation [online]. 2007. Available from: http://www.stkc.go.th/taxonomy/term/144?page=4 [2012, April]

[24] Philips, J.C., and Lucovsky, G. Fundamental Optical Spectra. Bonds and bands in semiconductors. pp 154-183. NY: Momentum Press, 2009.

[25] Wikipedia. Photoemission spectroscopy [online]. 2011. Available from: http://en.wiki pedia.org/wiki/Photoemission_spectroscopy. [2012, April].

[26] Michigan State University, Optical Spectroscopy and Instrumentation [online]. Available from: http://www.cem.msu.edu/~cem333/Week03.pdf. [2012, April].

[27] Gaponenko, S.V. Electron states in an ideal nanocrystal. Optical properties of semiconductor nanocrystals. pp 27-54. UK: Cambridge University Press, 1998.

[28] Tsidilkovskii, I. M. Band Structure of Semiconductors. Moscow: Nauka, 1978.

[29] Baldereshi, A., and Lipari, N. O. Hole Hamiltonian in spherical approximation. Phys. Rev. B 1973: 2697-701.

[30] Xia, J. B. Electronic states in zero-dimensional quantum wells. Phys. Rev. B 1989: 8500-7.

[31] Sweeny, M., and Xu, J. Hole energy levels in zero-dimensional quantum balls. Solid State Comm. 1989: 301-4.

[32] Sercel, P. C., and Vahala, K. J. Analytical formalism for determining quantum-wire and quantum-dot band structure in the multiband envelop-function approximation. Phys. Rev. B 1990: 3690-3710.

[33] Pan, J. L. Oscillator strengths for optical dipole interband transitions in semiconductor quantum dots. Phys. Rev. B 1992: 4009-19.

[34] Koch, S. W., Hu, Y. Z., Fluegel, B., and Peyghambarian, N. Coulomb effects and optical properties of semiconductor quantum dots. J. Cryst. Growth. 1992: 592-7.

[35] Takagahara, T., and Takeda, K. Theory of the quantum confinement effect on excitons in quantum dots of indirect gap materials. Phys. Rev. B 1992: 15578-83.

[36] Ekimov, A. I. et al. Absorption and intensity-dependent photoluminescence measurement on CdSe quantum dots: Assignment of the first electronic transitions. J. Opt. Soc. Amer. B 1993: 100-10.

[37] Lefebvre, P., Richard, T., Mathieu, H., and Allegre, J. Influence of spin-orbit split-off band on optical properties of spherical semiconductor nanocrystals. The case of CdTe. Solid State Comm. 1996: 303-6.

[38] Nomura, S., and Kobayashi, T. Nonparabolicity of the conduction band in CdSe and CdSSe semiconductor microcrystallites. Solid State Comm. 1991: 677-80.

[39] Rama Krishna, M. V., and Friesner, R. A. Quantum confinement effects in semiconductor clusters. J. Chem. Phys. 1991: 8309-21.

[40] Gaponenko, S.V. Growth of nanocrystals. Optical properties of semiconductor nanocrystals. pp 55-71. UK: Cambridge University Press, 1998.

[41] Ekimov, A. I., Efros, Al. L., and Onushchenko, A. A. Quantum size effect in semiconductor microcrystals. Solid State Comm. 1985: 921-4.

[42] Potter, B. G., and Simmons, J. H. Electronic states of semiconductor clusters: Homogeneous and inhomogeneous broadening of the optical spectrum. Phys. Rev. B 1988: 10838-45.

[43] Liu, L. C, and Risbud, S. H. Quantum dot size-distribution analysis and precipitation stages in semiconductor doped glasses. J. Appl. Phys. 1990: 28-32.

[44] Rossetti, R., Nakahara, S., and Brus, L. E. Quantum size effect in the redox potentials, resonance Raman spectra, and electronic spectra of CdS crystallites in aqueous solution. Chem. Phys. 1983: 1086-88.

[45] Weller, H. et al. Photochemistry of colloidal semiconductors. Onset of light absorption as function of size of small CdS particles. Chem. Phys. Lett. 1986: 557-560.

[46] Misawa, K., Yao, H., Hayashi, T., and Kobayashi, T. Size effects on luminescence dynamics of CdS microcrystallites embedded in polymer films. Chem. Phys. Lett. 1991: 113-8.

[47] Misawa, K., Yao, H., Hayashi, T., and Kobayashi, T. Superradiance quenching by confined acoustic phonons in chemically prepared CdS microcrystallites. J. Chem. Phys. 1991: 4131-40.

[48] Woggon, U. et al. Electro-optic properties of CdS embedded in a polymer. Phys. Rev. B 1993: 11979-86.

[49] Murray, C. B., Norris, D. J., and Bawendi, M. G. Synthesis and characterization of nearly monodisperse CdE (E=S, Se, Te) semiconductor nanocrystallites. J. Am. Chem. Soc. 1993: 8706-15.

[50] Nogami, M., Nagasaka, K., and Takata, M. CdS microcrystal-doped silica glass prepared by the sol-gel process. J. Non-Cryst. Sol. 1990: 101-6.

[51] Minti, H., Eyal, M., Reisfeld, R., and Bercovic, G. Quantum dots of cadmium sulfide in thin glass films prepared by sol-gel technique. Chem. Phys. Lett. 1991: 277-82.

[52] Spanhel, L., Arpac, E., and Schmidt, H. Semiconductor clusters in the sol-gel process: synthesis and properties of CdS nanocomposites. J. Non-Cryst. Sol. 1992: 657-62.

[53] Mathieu, H. et al. Quantum confinement effects of CdS nanocrystals in a sodium borosilicate glass prepared by the sol-gel process. J. Appl. Phys. 1995: 287-93.

[54] Wang, Y, Herron, N., Mahler, W., and Suna, A. Linear and nonlinear optical properties of semiconductor clusters. J. Opt. Soc. Am. B 1989: 808-13.

[55] Gurevich, S. A., Ekimov, A. I., Kudryavtsev, I. A., Osinskii, A. V., Skopina, V. I., and Chepik, D. I. Fabrication and study of SiO2 films activated with CdS nanocrystals. Semiconductor 1992: 102-6.

[56] Borrelli, N. F, Hall, D. W, Holland, H. J., and Smith, D. W. Quantum confinement effects of semiconducting microcrystallites in glass. J. Appl. Phys. 1987: 5399-5409.

[57] Gaponenko, S. et al. Nonlinear-optical properties of semiconductor quantum dots and their correlation with the precipitation stage. J. Opt. Soc. Amer. B 1993: 1947-55.

[58] Bawendi, M. G., Kortan, A. R., Steigerwald, M. L., and Brus, L. E. X-ray structural characterization of larger CdSe semiconductor clusters. J. Chem. Phys. 1989: 7282-5.

[59] Murray, C. B., Norris, D. J., and Bawendi, M. G. Synthesis and characterization of nearly monodisperse CdE (E=S, Se, Te) semiconductor nanocrystallites. J. Am. Chem. Soc. 1993: 8706-15.

[60] Hodes, G., Albu-Yaron, A., Decker, E, and Motisuke, P. Three-dimensional quantum-size effect in chemically deposited cadmium selenide films. Phys. Rev. B 1987: 4215-21.

[61] Potter, B. G., and Simmons, J. H. Quantum confinement effects in CdTe-glass composite thin films produced using rf magnetron sputtering. J. Appl. Phys. 1990: 1218-24.

[62] Liu, L-C, Kim, M. J., Risbud, S. H., and Carpenter, R. W. High-resolution electron microscopy and microanalysis of CdS and CdTe quantum dots in glass matricies. Philosoph. Mag. B 1991: 769-76.

[63] Ochoa, O. R., Colajacomo, C, Witkowski, E. J., Simmons, J. H., and Potter, B. J. Quantum confinement effects on the photoluminescence spectra of CdTe nanocrystallites. Solid State Comm. 1996: 717-21.

[64] Bandaranayake, R. J., Wen, G. W, Lin, J. Y, Jiang, H. X., and Sorensen, C. M. Structural phase behavior in II-VI semiconductor nanoparticles. Appl. Phys. Lett. 1995: 831-3.

[65] Neto, J. A. M., Barbosa, L. C, Casar, C. L., Alves, O. L., and Galembeck, F. Quantum size effects on CdTexSi_x semiconductor-doped glass. Appl. Phys. Lett. 1991: 2715-7.

[66] Chestnoy, N., Hull, R., and Brus, L. E. Higher excited electronic states in clusters of ZnSe, CdSe, and ZnS: Spin-orbit, vibronic, and relaxation phenomena. J. Chem. Phys. 1986: 2237-12.

[67] Goncharova, O. V., and Sinitsyn, G. V. Optical characteristics of vacuum deposited quantum-size structures of II-VI compounds. Izv. Akad. Nauk BSSR 1990: 21-8.

[68] Kortan, A. R. et al. Nucleation and growth of CdSe on ZnS quantum crystallites seeds, and vice versa, in inverse micelle media. J. Am. Chem. Soc. 1990: 1327-32.

[69] Bhargava, R. N., Gallagher, D., Hong, X., and Nurmikko, A. Optical properties of manganese-doped nanocrystals of ZnS. Phys. Rev. Lett. 1994: 416-9.

[70] Illing, M. Lateral quantization effects in lithographically defined CdZnSe/ZnSe quantum dots and quantum wires. Appl. Phys. Lett. 1995: 124-6.

[71] Zylberajch, C, Ruaudel-Teixier, A., and Barraud, A. Properties of inserted mercury sulphide single layers in a Langmuir-Blodgett matrix. Thin Solid Films 1989: 9-14.

[72] Lowisch, M., Rabe, M., Stegeman, B., Henneberger, R, Grundmann, M., Tuerck, V., and Bimberg, D. Zero-dimensional excitons in (Zn,Cd)Se quantum structures. Phys. Rev. B 1996: R11074-7.

[73] Amornsuk Chanagul. Effects of types of anions and cosurfactants on ZnS nanoparticle synthesis in microemulsion. Master's thesis, Department of

Chemical Engineering, Faculty of Engineering, Chulalongkorn University, 2005.

[74] Promod Kumar, and Mittal, K.L. Handbook of Microemulsion Science and Technology. Marcel Dekker, 1999.

[75] Lopez-Qiontela, M.A., Tojo C., Blanco, M.C., Garcia Rio, L., and Leis, J.R. Microemulsion dynamics and reactions in microemulsions. Curr. Opin. Colloid Interface Sci. 2004: 264-278.

[76] Holmberg, K. Surfactant-templated nanomaterials synthesis. J. Colloid Interface Sci. 2004: 355-364.

[77] Erikkson, S., Nylen, U., Rojas, S., and Boutonnet, M. Preparation of catalysts from microemulsions and their applications in heterogeneous catalysis. Appl. Catal. A 2004: 207-219

[78] Wikipedia. Microemulsion [Online]. 2012. Available from: http://en.wikipedia.org/ wiki/Microemulsion [2012, April]

[79] Wikipedia. Polymerization [online]. 2012. Available from: http://en.wikipedia.org/ wiki/Polymerization. [2012, April]

[80] Javier Cruz, C. Advanced cure monitoring and analysis for optimization of thermoset resin processes, Doctoral thesis, Wisconsin-Madison University, 2008

[81] Mall, M., Kumar, P., Chand, S., and Kumar. L. Influence of ZnS quantum dots on optical and photovoltaic properties of poly (3-hexylthiophene). Chem. Phys. Lett. , 2010: 236–240.

[82] Wageha, S., Zhao, S., Linga, B., and Rong, X. Growth and optical properties of colloidal ZnS nanoparticles. J. Cryst. Growth., 2003: 332–337.

[83] Barman, B., and Sarma ,K.C. luminescence properties of ZnS quantum dots embedded in polymer matrix, Department of Instrumentation and USIC. Gauhati University, (March 2011):171 – 176.

[84] James, H., and Ender, S. Morphological control of particles. Curr. Opin. Colloid Interface Sci., 2000: 160-167.

[85] Sigma product information sheet. Triton X-100 [PDF online]. Available from: www.snowpure.com/docs/triton-x-100-sigma.pdf [2012, April].

[86] Ashok, K.G., Aparna, G., and Sonalika, V. Microemulsion-based synthesis of nanocrystalline materials. Chem. Soc. Rev., 2010: 474-485.

APPENDICES

APPENDIX A
THE ZNS NANOPARTICLE CRYSTALLITE SIZE APPROXIMATION FROM TEM IMAGES

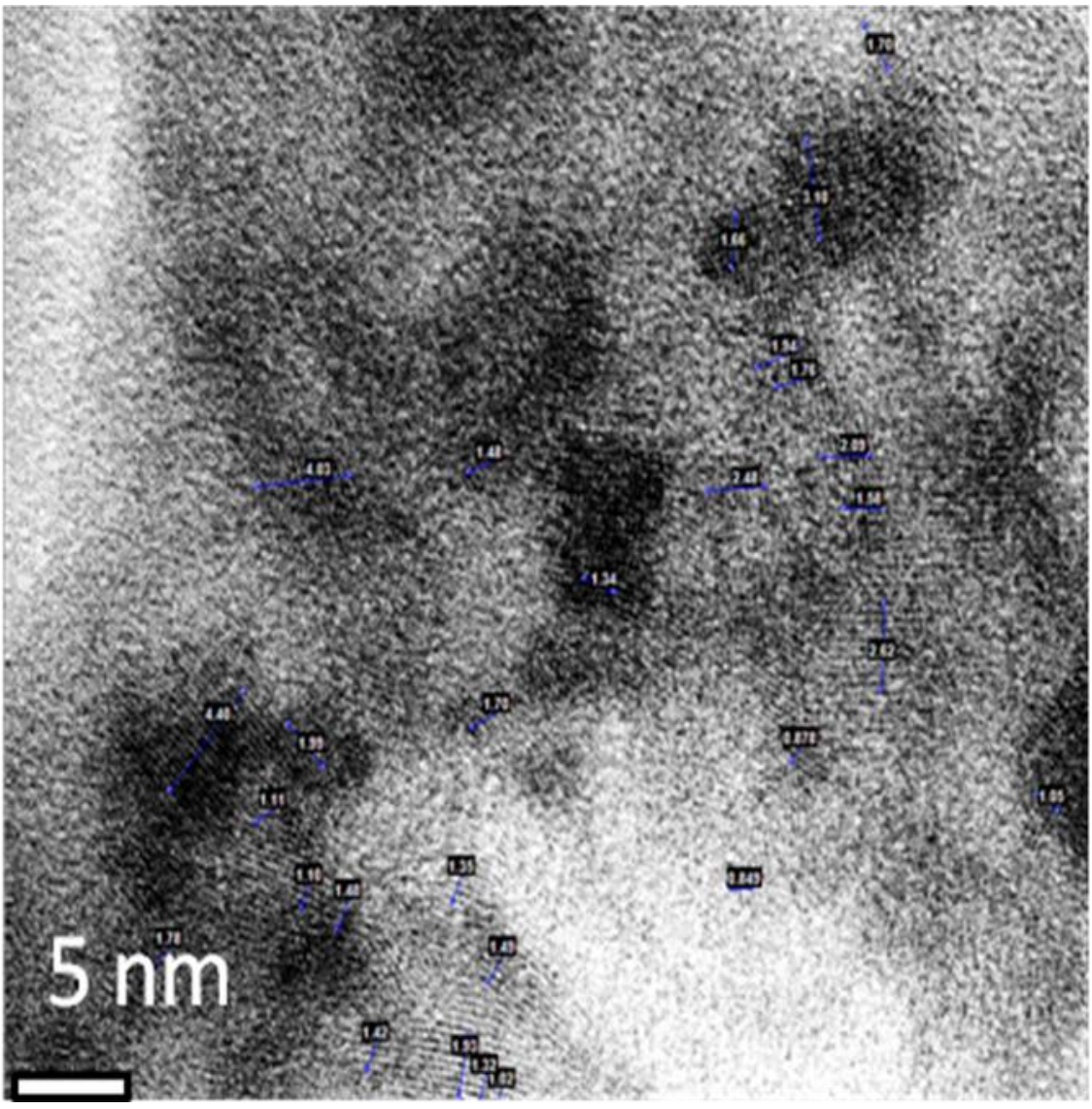

Figure A.1 TEM image of C01W3 ZnS nanoparticle

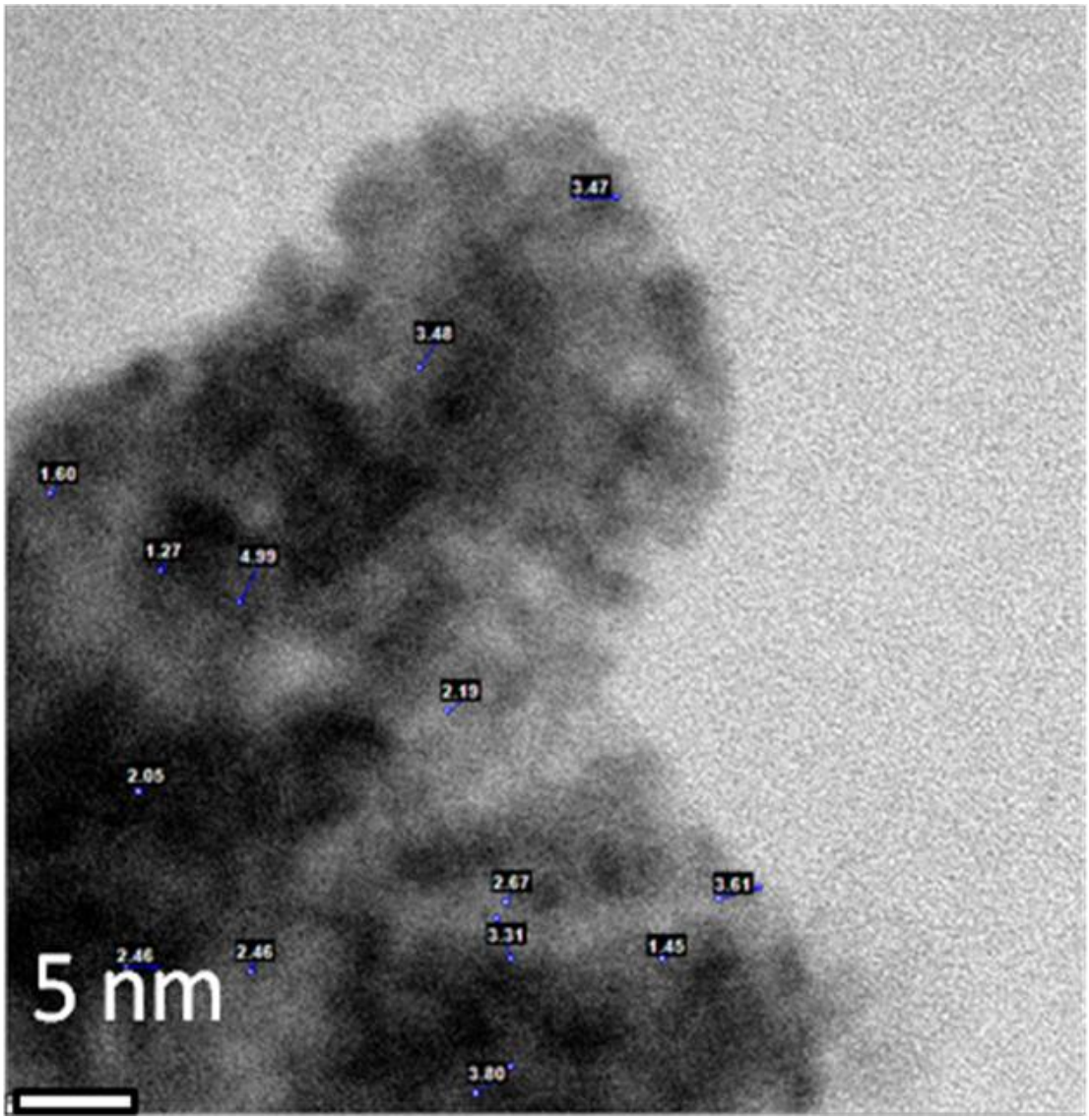

Figure A.2 TEM image of C05W3 ZnS nanoparticle

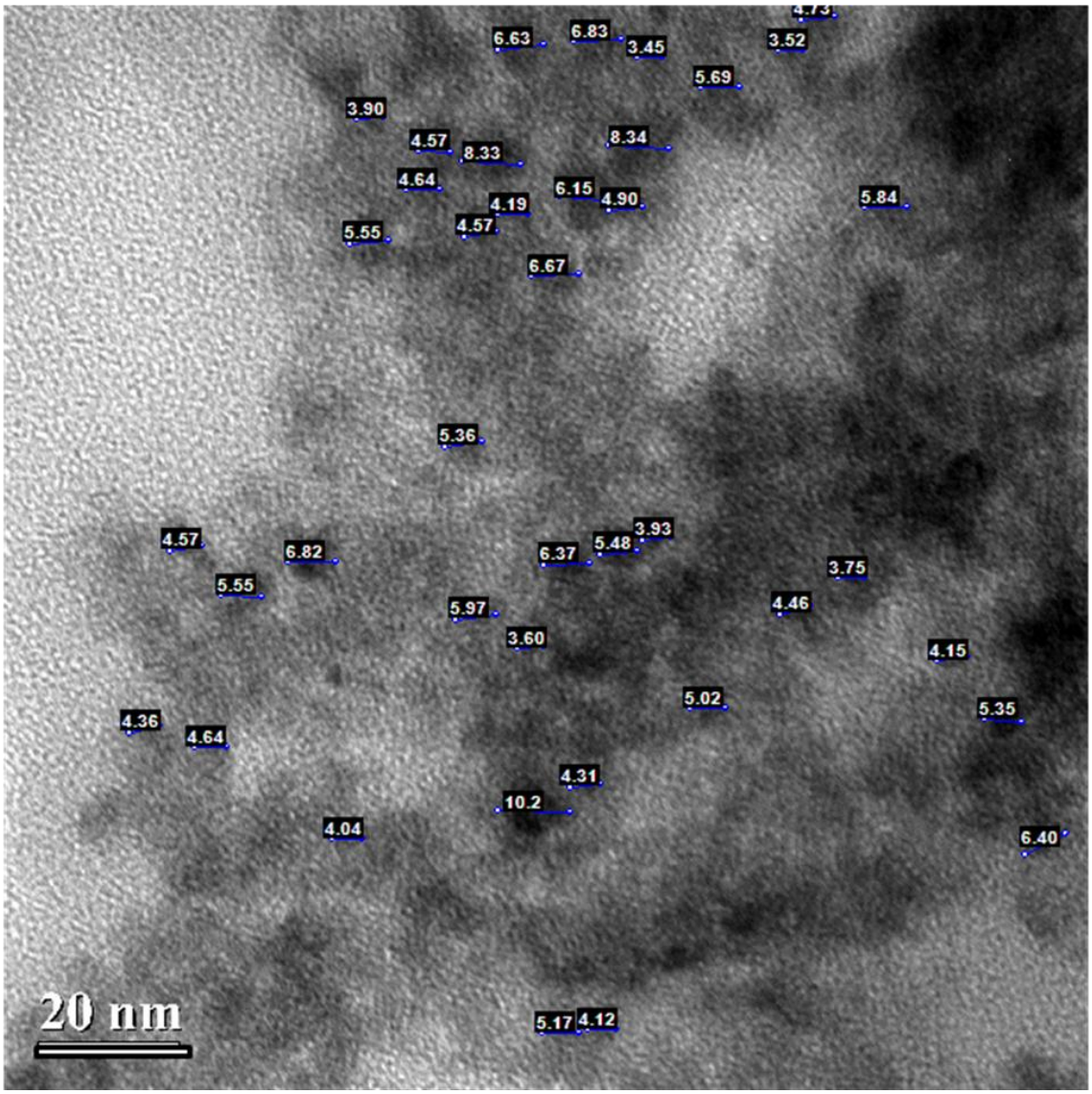

Figure A.3 TEM image of C05W7 ZnS nanoparticle

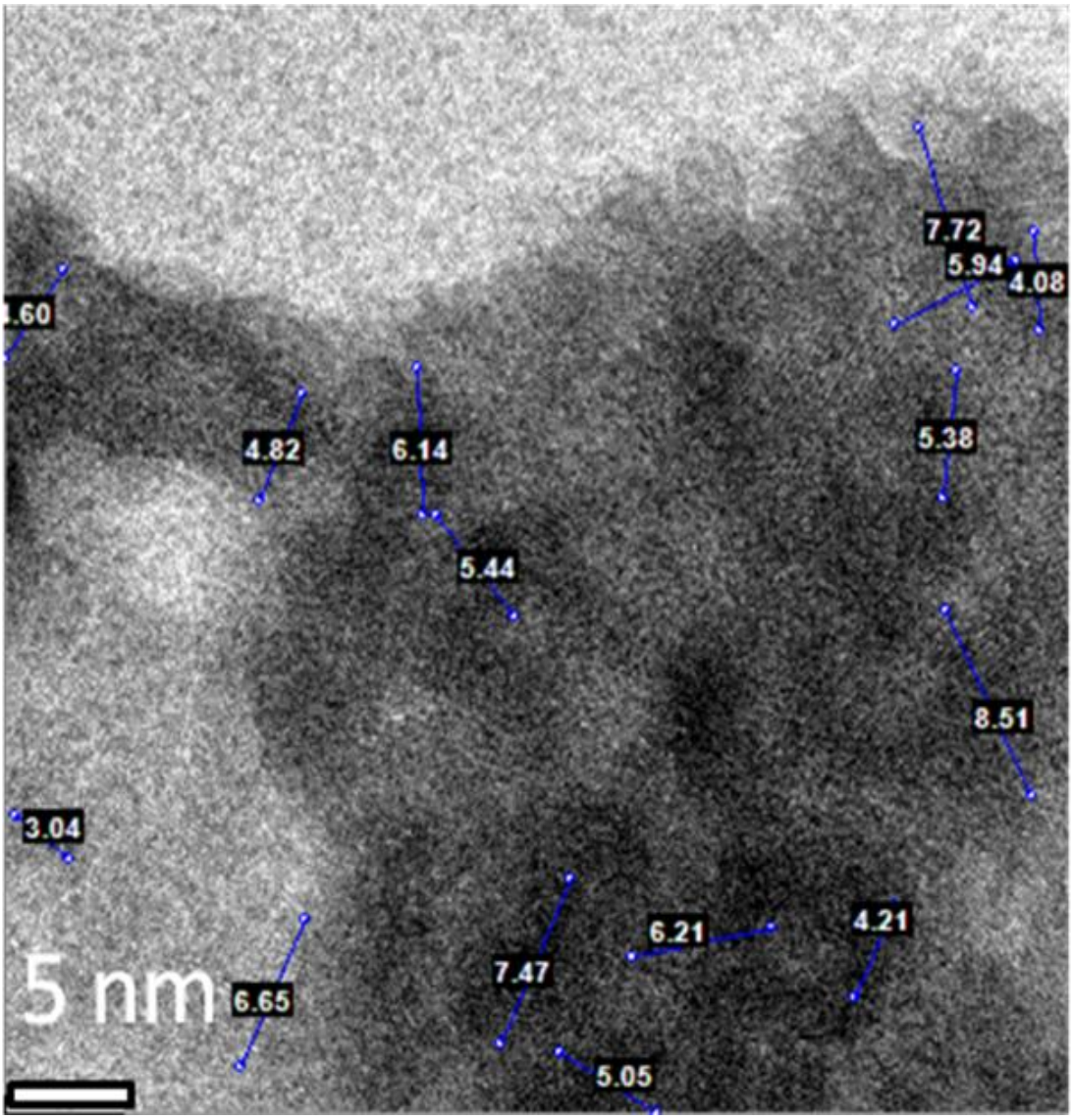

Figure A.4 TEM image of C05W9 ZnS nanoparticles

Table A.1 The approximately average crystallite size

number	C01W3	C05W3	C05W7	C05W9
1	6.72	2.02	4.90	12.95
2	4.74	2.16	6.15	16.73
3	2.5	2.33	4.58	6.12
4	1.69	2.34	8.34	6.31
5	3.51	2.16	8.33	6.53
6	4.57	2.46	6.40	5.03
7	2.44	2.84	4.05	4.82
8	2.46	2.48	3.60	5.86
9	1.21	2.24	4.31	4.04
10	1.19	2.54	7.63	6.18
11	1.27	1.94	3.45	7.08
12	0.85	2.54	5.69	4.80
13	1.44	3.43	5.35	7.73
14	1.44	3.01	6.98	8.53
15	1.31	2.32	4.46	6.23
16	0.94	2.78	3.52	7.19
17	1.15	3.31	4.73	9.73
18	1.06	2.16	6.83	4.37
19	1.34	2.24	4.57	6.63
20	1.4	2.19	4.65	4.27
21	1.47	2.61	3.93	6.92
22	1.53	2.32	6.37	6.82
23	1.81	2.02	10.19	5.46
24	1.97	2.08	4.64	6.33
25	3.58	2.09	3.90	9.23
26	4.16	2.18	5.55	5.05
27	0.71	3.94	5.55	4.21
28	3.29	2.09	4.20	6.21
29	1.1	2.24	6.57	7.47
30	2.84	3.34	6.67	6.65
31	1.82	3.11	5.84	4.60
32	1.92	2.25	5.02	5.94
33	1.73	2.20	5.48	4.08
34	1.51	3.05	3.75	7.72
35	2.7	2.02	4.15	5.38
36	1.58	2.11	4.36	8.51
37	1.51	2.02	6.82	3.04
38	2.47	3.94	4.12	5.44
39	1.42	2.09	5.17	4.82
40	1.21	2.24	5.36	6.14
Avg. size	2.08	2.49	5.40	6.53

APPENDIX B

XRD SPECTRA OF ZNS NANOPARTICLES

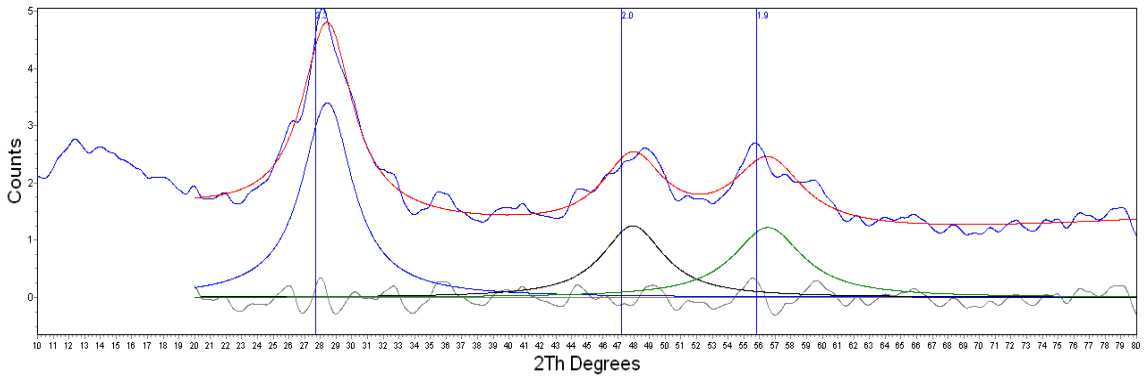

Figure B.1 XRD spectra of C01W3 ZnS nanoparticle

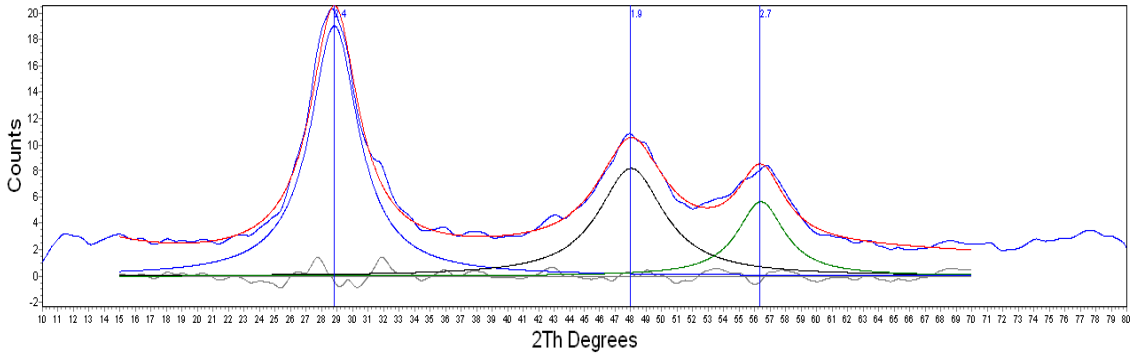

Figure B.2 XRD spectra of C01W7 ZnS nanoparticle

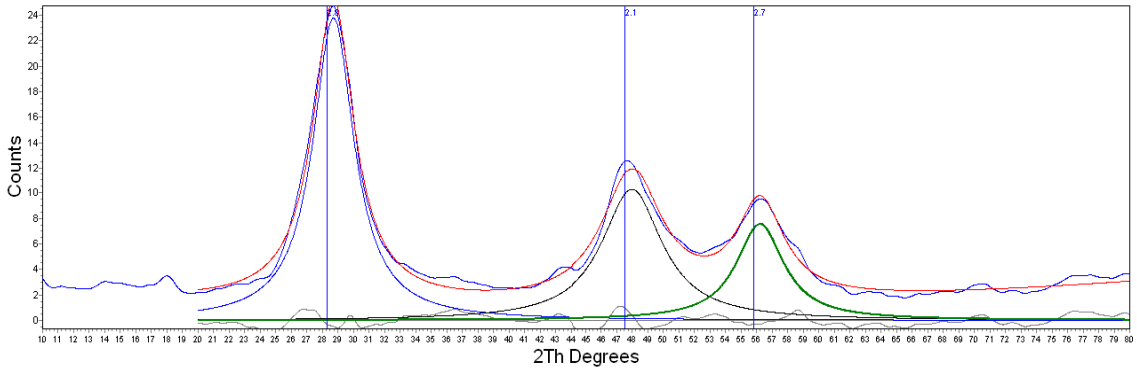

Figure B.3 XRD spectra of C01W9 ZnS nanoparticle

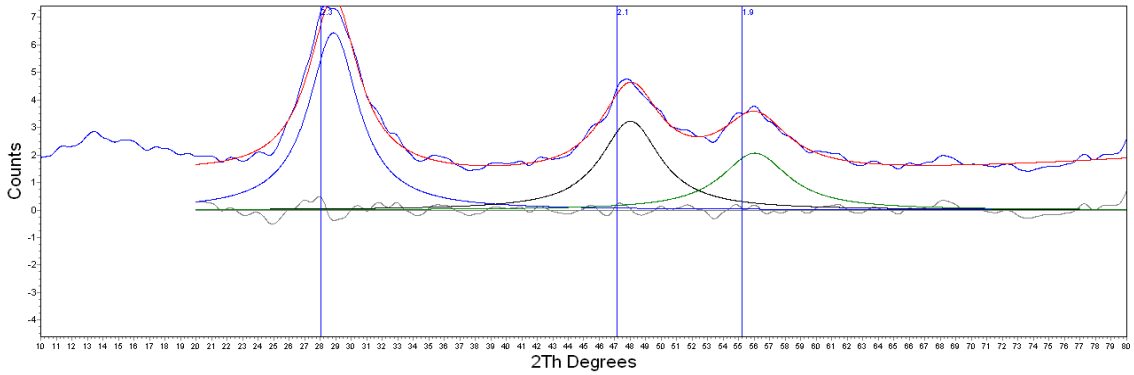

Figure B.4 XRD spectra of C05W3 ZnS nanoparticle

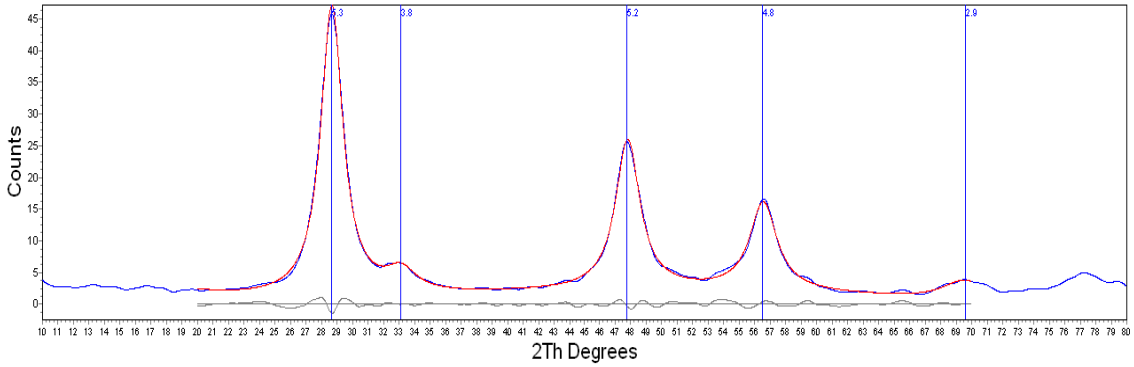

Figure B.5 XRD spectra of C05W7 ZnS nanoparticle

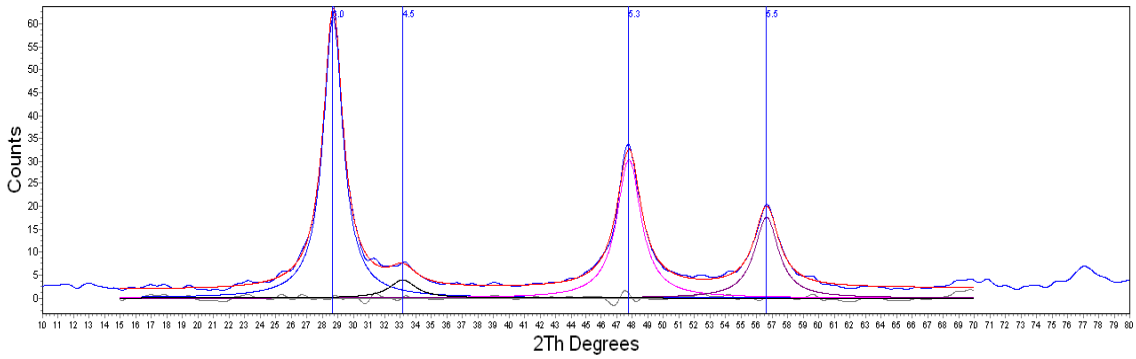

Figure B.4 XRD spectra of C05W9 ZnS nanoparticle

APPENDIX C
SOLAR CELL ELECTRICAL DATA

Table C.1 Electrical current, Voltage and power generation

Condition	I (μA)	V (mV)	P (nW)
C01W3	0.81	177.4	143.694
C01W7	0.77	165.9	127.743
C01W9	0.71	152.9	108.559
C05W3	0.8	160.6	128.48
C05W7	0.74	161.5	119.51
C05W9	0.68	146.4	99.552

APPENDIX D

EDS Spectra

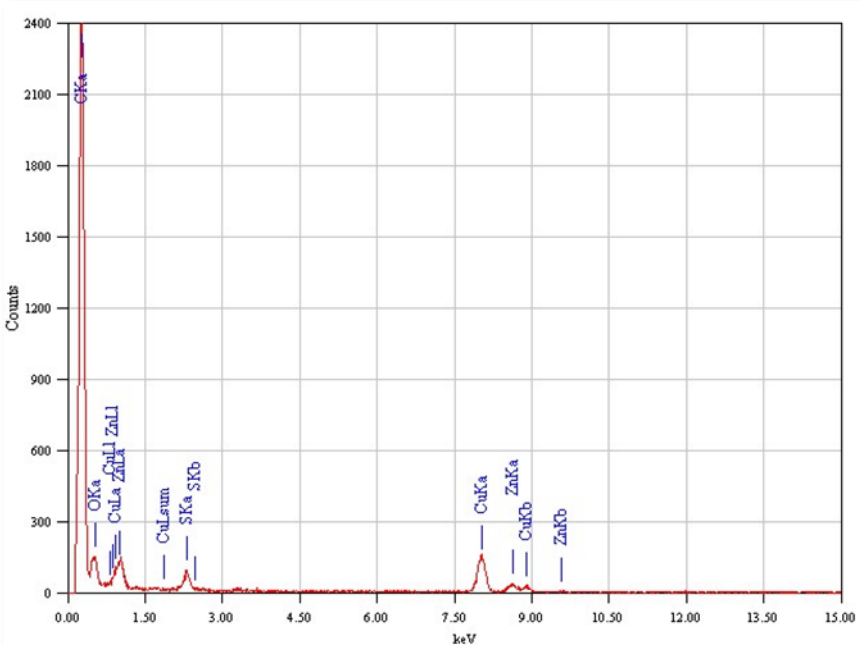

Figure D.1 EDS spectrum of C01W3 ZnS nanoparticle

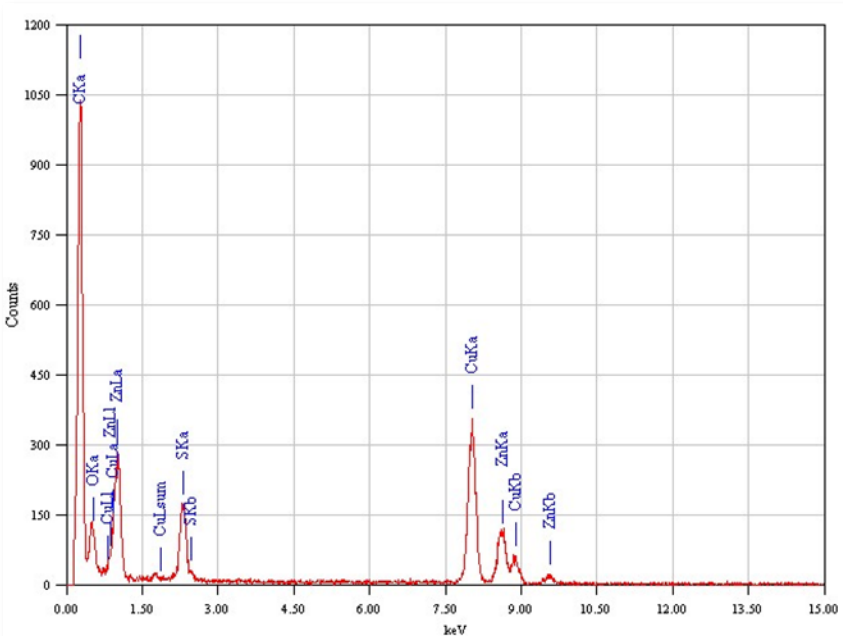

Figure D.2 EDS spectrum of C01W7 ZnS nanoprticle

APPENDIX E
LIST OF PUBLICATIONS

Kanokwan Wangno, Sitthisuntorn Supothina, Wattana Ratismith, Pitchnaree Maneeratanakul, Warisa Tiravanich, and Tawatchai Charinpanitkul. “Synthesis of nano-sized ZnS by reversed micelle of Triton X-100 in cyclohexane”. (the proceeding of Pure and Applied Chemistry International Conference 2012 (PACCON 2012), Chieng mai)

Kanokwan Wangno, Sitthisuntorn Supothina, Wattana Ratismith, and Tawatchai Charinpanitkul. “Synthesis of nano-sized zinc sulfide via micro-emulsion route”. (the proceeding of TIChE international conference 2011, Songkhla)

VITA

Kanokwan Wangno was born on June 8, 1987 in Roi-et, Thailand. She studied at Ubonratchathani University in Chemical Engineering, Faculty of Engineering and got graduated with GPA 3.49 in March 2010. She continued her Master's degree in Chemical Engineering, Chulalongkorn University in the Center of Excellence in Particle Technology laboratory group in June 2010.